Investigating Active Stabilization of Rocket using Canards
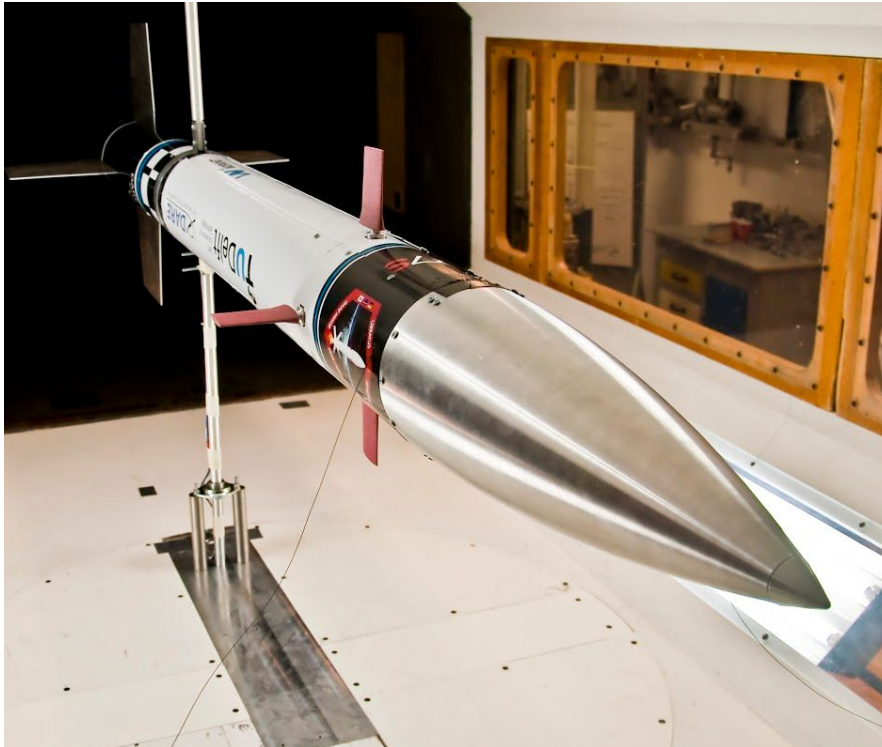

Image obtained from Delft Aerospace Rocket Engineering Team (Wind Tunnel Tests Conducted in 2014)[3]

Svena Yu
Christian Wilson

Project Sponsors:
UBC Rocket

Project 2012
Engineering Physics 459
Engineering Physics Project Laboratory
The University of British Columbia
April 8, 2020

Table of Contents

Executive Summary

UBC Rocket is designing and building a liquid propelled rocket, called Whistler-Blackcomb, to reach the Karman line at an altitude of 100 kilometers. Maintaining a stable rocket throughout it's flight path is critical for a safe and successful launch. This report focuses on investigating the effectiveness of canards - an aerodynamic element near the top of a rocket - as an active stabilization device to control the rocket's roll rate. Two fins are sufficient to achieve control in the roll axis.

A smaller rocket provided by the sponsor will be used as a scaled down test bed to verify our initial calculations. A static module instrumented with load cells to measure the aerodynamic load produced by each fin in a wind tunnel environment was designed and built. Simulations were ran and showed high confidence that at 10 degrees angle of attack, a low airspeed of 50m/s can sufficiently generate enough torque to control the rocket. Wind tunnel tests on the prototype need to be conducted to verify this claim and further analysis is needed to characterize the behaviour of canards for airspeeds closer to Mach 1.

Introduction

The project sponsor UBC Rocket is a student Engineering Design Team based at the University of British Columbia's Vancouver campus. Established in 2017, UBC Rocket has been consistently building and launching amateur rockets at the annual Spaceport America competition that takes place in New Mexico, USA. Out of the three rockets that have been built and launched, the first rocket achieved first place in the 10,000ft category and the third achieved fourth place in the 30,000ft category.

UBC Rocket has a team that is currently working to design and build a rocket, named Whistler-Blackcomb, to reach the Karman line using a liquid propulsion system. The Karman line is the internationally defined boundary between Earth and outer space at an elevation of 100 kilometers (300,000 ft) above the Earth's surface.

Background and Significance

The Whistler Blackcomb rocket is designed to have large passively stabilized fins near the engine. These fins help to damp out aerodynamic disturbances like winds, gusts, as well as other contributing elements of instability like unequal mass balances. This is a feature commonly used on amateur solid or hybrid rockets as well. However, liquid propulsion rockets have an additional challenge of liquid propellant slosh in the tanks during flight. This phenomenon happens due to "inertial waves"[19] that form on the surface of the propellant when the rocket experiences sudden impulses during takeoff and angular acceleration about its longitudinal axis during flight.

The sloshing of the propellant tanks can enter into a positive feedback loop with the system dynamics of the rocket[19]. A small roll can initiate propellant slosh, which causes the roll to accelerate and the rocket to oscillate about the pitch or yaw axis, giving more energy to the propellant slosh. This can cause fuel or oxidizer supply to the engine to fluctuate and exert high levels of stress to the rocket's structural airframe.

Propellant slosh is the reason that the Whistler Blackcomb team has identified the importance of controlling the roll of the rocket in relation to minimizing the initiation of slosh in the tanks.
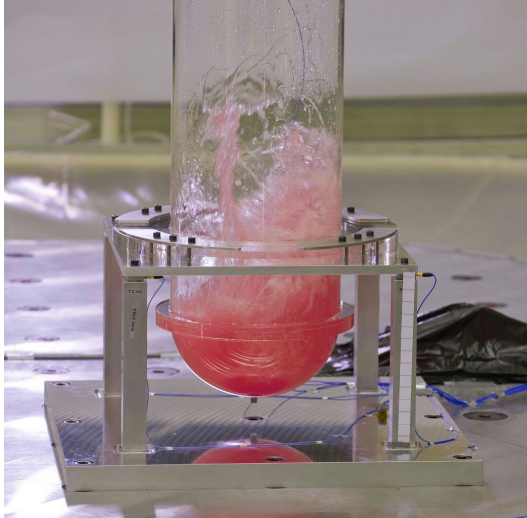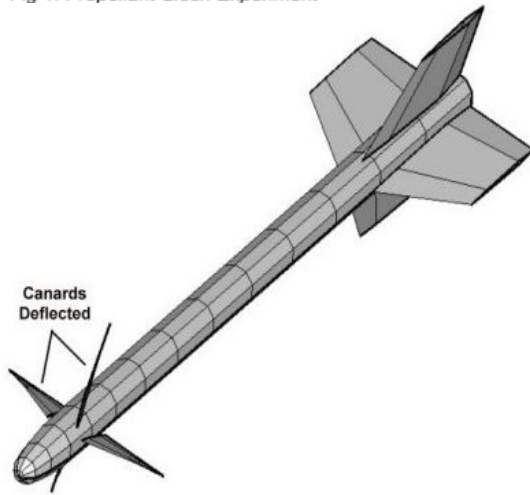
UBC Rocket has identified the potential of canards - an aerodynamic element that can be placed near the top of a rocket - to use as Whistler-Blackcomb's active stabilization system and wishes to verify the feasibility of this idea.

Canards are small fins typically used as aerodynamic control surfaces that have been investigated as far back as the Wright Brothers. They are commonly used in guiding missiles that travel up to Mach 3.5 speeds and are used to control the pitch, roll and yaw of these missiles[2]. Another usage is in the active stabilization of amateur solid rocket projects and has been found to be effective stabilization mechanisms[15], with a drawback of being unpredictable beyond subsonic speeds.

The AIM-9M Sidewinder[21] is a widely produced short range air-to-air missile propelled by a solid grain motor that has canards as its main guidance mechanism.

Fig 1. Propellant Slosh Experiment [20]

Canards Deflected

Fig 2. Canard deflections on an AIM-9M Sidewinder [21]

Project Objectives

We are interested in investigating the use of canards as effective control surfaces for the Whistler Blackcomb liquid propulsion rocket.

To qualify if canards are effective, the baseline performance metric the canard system needs to be able to meet is to generate enough lift to create the required counter torque such that the roll of the rocket can be controlled.

Further performance metrics that we are interested in are the packaging of the canard deflection mechanism and the coupling effects between the canard and other aerodynamic elements of the rocket to ensure that the canard is not adding significant instability or drag to the system.

To evaluate our objectives, we plan to design and build a prototype and conduct wind tunnel tests to obtain empirical data.

Scope and Limitations

The scope originally included building a fully functional canard module that would be able to actively stabilize a smaller prototype rocket platform during a wind tunnel test and included simulation work on control inputs necessary. This was deemed to be too large of a scope and in discussions with UBC Rocket and the Project Lab staff, was narrowed down to the table below:

Table 1: Requirements and Possible Results for each Module

	Dynamic Module	Static Module
Servos	✔	X
Gyroscope	✔	X
Strain Gauges	X	✔
Control Algorithm	✔	X
Torque vs Velocity vs CFD	X	✔
Transient Response	✔	X
Test stabilization from induced roll	?	X

We will start with designing and building the Static Module. The Static Module is intended to be used to compare the aerodynamic lift generated in the wind tunnel test to that predicted by the simulation model at AOA from 0° to 10°. The AOA of the fin is adjusted in situ statically before each test according to a template. This data will be used to do a first pass evaluation of the feasibility and will help to refine the fin model.

The Dynamic Module has servo actuation and gyroscopes and will be able to receive input of the rocket's position and output the new position of the fin. The Dynamic Module can be tested in a wind tunnel with a rotary mount (such as the University of Washington's 3x3 Low Speed Wind Tunnel) and can be used to test active stabilization code at low speeds.

These two modules are intended to fit into the same external envelope so that installation and removal is simplified.

Limitations

Table 2: Project Limitations

Wind Tunnel Speeds	One of the key limitations is the lack of access to a high speed wind tunnel (more than ~90m/s). The Parkinson Wind Tunnel available to us has a maximum airspeed of 30m/s. Compressibility starts becoming more significant and simulation results can be expected to deviate from the empirical results at around 90~100m/s. We have no way of experimentally verifying this.We would have to rely solely on the integrity of our aerodynamic simulation to characterize the system at high speeds.
Wind Tunnel Size	Due to the constrained size of the wind tunnel available to use in school (Parkinson Wind Tunnel), we will only be able to test with the nose cone attached to the upper body tube that houses the modules. The rear fins will be too large and will disturb the flow in the wind tunnel. This will be not as accurate of a test as there are interactions between the tail and the canards that are difficult to model.
Limited Region of Effective Control	The Whistler Blackcomb Rocket hits supersonic speed at about 11 seconds into flight (Flight Profile is detailed in Appendix A) and accelerates up to Mach 4 thereafter so the effective control period may only be limited to the first 10 seconds.
Lack of Existing Data	There is very little publicly available data on the roll rate of a liquid propulsion rocket. The data on how propellant slosh affects the system of a rocket is limited as well, so obtaining an accurate upper boundary of the rocket's roll rate is difficult. Estimates that are too conservative will make the system unnecessarily heavy and inefficient.

Theory of Fundamentals

Canards mount to the rocket airframe and are able to rotate about a central pivot point. This rotation changes the angle of attack (AOA) which can be used to control the lift generated by each canard. Using a combination of two canards allows control of the roll of the rocket. With four canards, all three - pitch, yaw, and roll - movements can be controlled.

In the four fin configuration, pitch can be achieved by angling two fins 180º apart symmetrically and yaw can be achieved with two other fins in the perpendicular plane symmetrically. Roll can be achieved with two opposing fins angled anti symmetrically. To control all three axis, the control parameters for each axis are superimposed together.

As AOA is increased, the coefficient of lift also increases (and so does parasitic drag). The relationship is roughly linear at small AOA[16].

$$C_L = 2\pi * A0A$$

This relationship decays quickly as the AOA reaches the stall angle and C_L goes to 0.
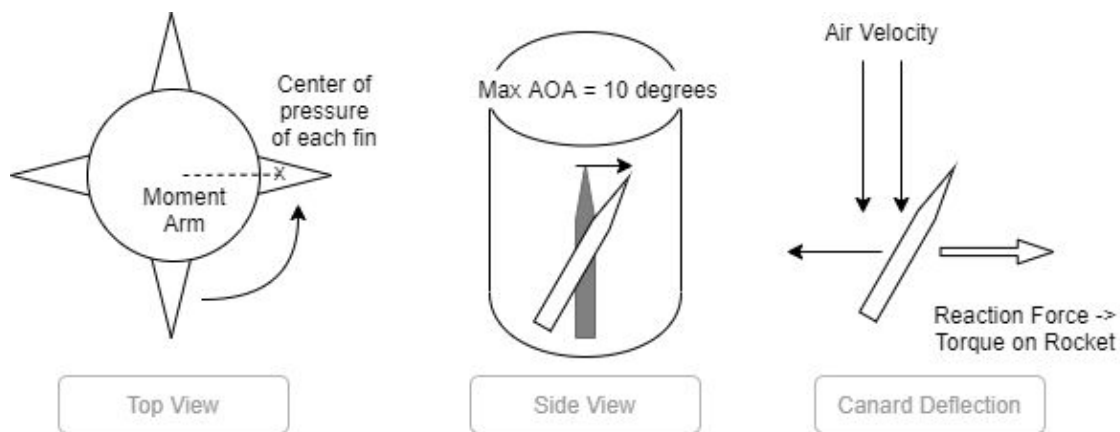

Fig 3. Diagram of canards system, explanation of forces from deflection

Assuming the canard to the rocket body's connection is infinitely stiff, we can relate the aerodynamic lift of the fin to the counter torque produced using a simple moment arm expression.

$$\tau = F_L * d$$

Where F_L refers to the lift force and d refers to the moment arm, which extends from the center of the rocket to the center of pressure of the fin.

The center of Pressure is the average location of aerodynamic pressure on a given surface. This is given by the following equation[16]:

$$c_p = \frac{\int xp(x)\,dx}{\int p(x)\,dx}$$

Coefficient of Lift for v < 100 m/s can be approximated by the following equation[18]:

$$C_L = \frac{2F_L}{\rho v^2 A}$$

Where ρ is the fluid density, v is the fluid velocity and A is the control surface area.

For v > 100m/s but still within the subsonic range (M<1), compressibility of the air plays a non negligible part in the fluid-solid interactions and can be accounted for using a compressibility factor[18]:

$$C_L = \frac{C_{L0}}{\sqrt{1-M^2}}$$

Where C_{L0} is the lift coefficient in incompressible flow.

As the flow structure changes dramatically beyond the transonic region, it is not within our scope to account for canard behaviour past the subsonic region.

When integrating the canard with the rocket body, we also need to account for the dynamic stability of the rocket. The rocket is considered dynamically stable if, at all stages of the flight,

the center of pressure is aft of the center of gravity. As the center of pressure tends to move higher up the rocket as the angle of attack increases, the "static margin" is often used to characterize the stability. The static margin is given by[18]:

$$Static\ Margin\ =\ \frac{X_{cp}-X_{cg}}{D_{max}}$$

$$1\ <Static\ Margin\ <2$$

Where X_{cp} and X_{cg} are the location of the center of pressure and the center of gravity located aft of the nose-cone tip. D_{max} is the largest diameter of the rocket.

Too little static margin and the center of pressure might creep forward of the center of gravity, causing aerodynamic disturbances to amplify. Too much static margin might increase the rocket's tendency to weathercock into the wind during flight, which is also undesirable.

The major contributions to the center of pressure are from the nose-cone and the rear fins. Adding canards to the top of the rocket will move the original center of pressure up closer to the center of gravity and care has to be taken to ensure that the rocket maintains an acceptable static margin.
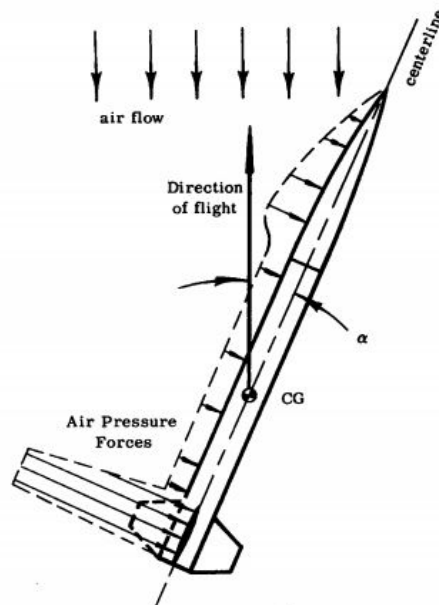

Fig 4. Aerodynamic Pressure distribution along rocket body[17].

Approach

As it is not practical to design for the large rocket (which is 8m tall and 0.5m in diameter), we have decided to use a smaller rocket (6.5" in diameter) as the test platform for our prototype static module assembly.

We start by quantifying the amount of counter torque to maintain a steady, controlled roll rate during flight. No useful data on roll acceleration rates for liquid propulsion rockets could be freely located searching the internet and browsing NASA archives.

A simplified approach uses publicly available data for amateur solid motor rockets. Referencing D.Walker & H.Hunt's (2016) project, a test launch of a solid rocket gave the following results[10]:

Table 3: Reference Rocket accelerations

Approximate Acceleration (with Gravity) in the first 2 seconds of flight	76.48 m/s^2
Approximate Roll Acceleration in the first 2 seconds of flight	5.24 rad/s^2

The Whistler Blackcomb rocket's flight path was simulated using ASTOS (a mission analysis tool supported by the European Space Agency) and within the first 2 seconds of flight, the acceleration of the rocket averages to 25.4 m/s^2, which is about a third of that experienced by the solid rocket cited above. We will expect the roll acceleration of the rocket to be much less than that experienced by a solid rocket. A conservative estimate for the angular acceleration for the liquid propulsion rocket is half of an equivalent solid rocket, so we will use $\alpha = 2.62 \ rad/s^2$ in our following calculations.

The counter torque necessary to prevent excessive roll is given by $\tau = I\alpha$. $I = \frac{1}{2}MR^2 = 0.5 * 576kg * 0.25^2 = 18.1 kgm^2$. We are approximating the rocket as a uniform density rod, which is a reasonable assumption as around 75% of the mass budget has been allocated for liquid propellants. Hence the torque necessary is estimated to be 47.16 Nm for the full scale rocket.

Hence, by simple dimensional analysis:

We apply a factor of $\frac{(prototype\ radius)^2}{(full\ scale\ radius)^2} * \frac{prototype\ rocket\ mass}{full\ scale\ rocket\ mass} = 0.00189$.

- Prototype radius = 3.25 in (8.255cm)
- Full scale radius = 25cm
- Prototype rocket mass (assuming same density as full scale, length of prototype rocket is 2m) = 15.7 kg
- Full scale rocket (8m in length) loaded mass = 576 kg

The conservative estimate for the amount of counter torque the prototype canard needs to exert on the rocket body is approximately **0.140 Nm.** This is the number we will be using in sizing our components.

Design

Mechanical Design

We first started off with designing the static module. The following key principles guided our design:

- Modularity
  - The mounting mechanism should be easily assembled and should be nearly identical for each fin.
- Symmetry
  - Symmetrically mounted fins are important to produce balanced forces about the longitudinal axis.
- Ease of access
  - During the wind tunnel test, we would need to adjust the angle of each canard fin to manually. We were careful to design the mounting mechanism of the static module such that the angle of the fin could be easily adjusted in situ.
- Ease of manufacturing

○ Due to the limited time of this project, we tried to minimize the number of components and features that needed to be custom machined, while still preserving the precision necessary to obtain useful data.

Design Constraints

The rocket body we are working with is the 2019 competition rocket of UBC Rocket, named "SkyPilot".
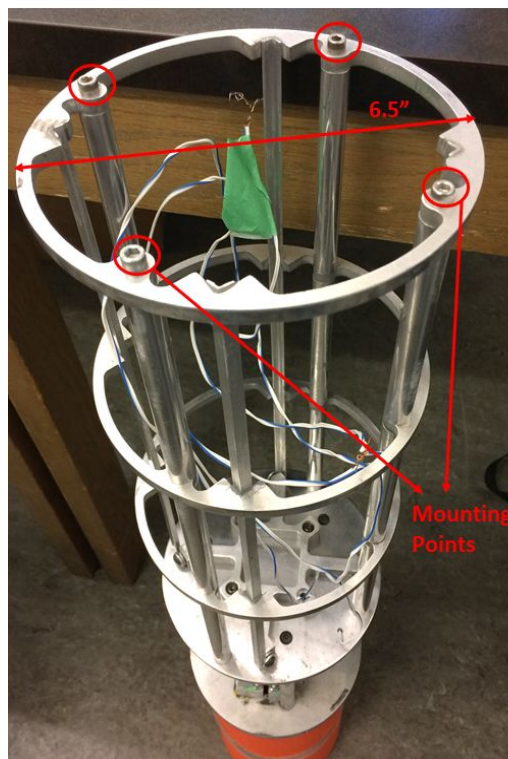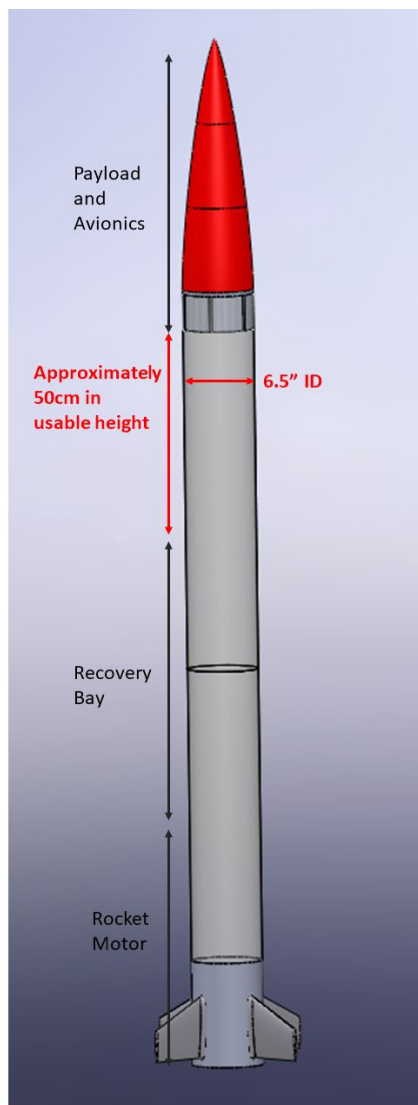

Fig 5. (far left) This is the high level diagram of the rocket and the section in red marks out the intended section to use to mount our canard assembly.

Fig 6. (left) This picture is the physical internal structure that sits inside the rocket body. The mounting points that our system will interface with and internal dimensions are shown.

The internal structure in the Skypilot rocket consists of flat aluminum plates stood off to make 5 platforms. The carbon fiber airframe skin is then slid over the internal structure and there is a simple locking mechanism to keep the carbon fiber body and aluminum platforms together.

As the airframe skin is a close sliding fit over the internal structure, our canard assembly must be within the boundary circle of 6.5" in diameter.

Fin Design

Our approach to designing the fin is to start with a simple shape, with parameters referenced from existing literature. A clipped delta shape was found to be quite common and performed well in subsonic speeds producing the lowest drag out of other fin shapes at 0° AOA[21].
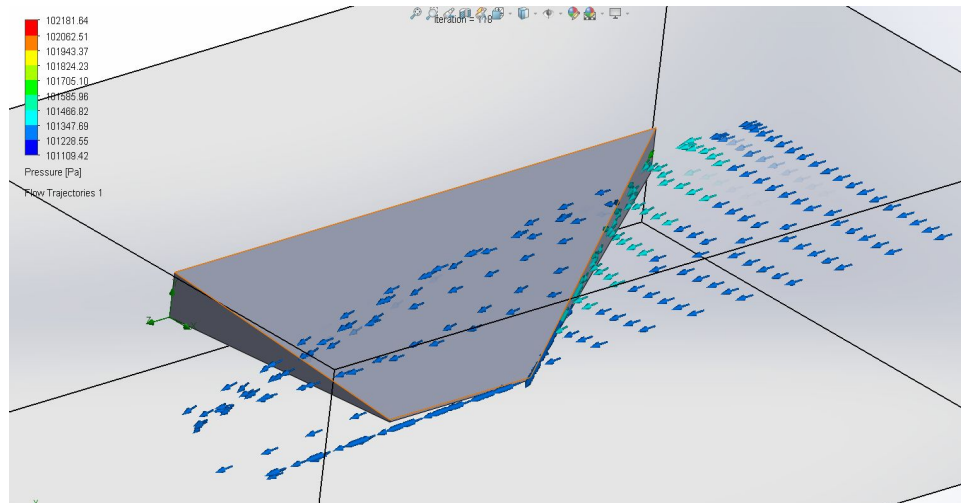

Fig 7. Solidworks flow simulation of initial flat plate design with a taper that narrows towards the shorter edge. The flow can be seen to be detaching from the surface of the plate. The small arrows represent local fluid velocity

Starting off with a simple flat plate with tapered ends and a clipped angle of 50°, the flow separates prematurely around 9° AOA.
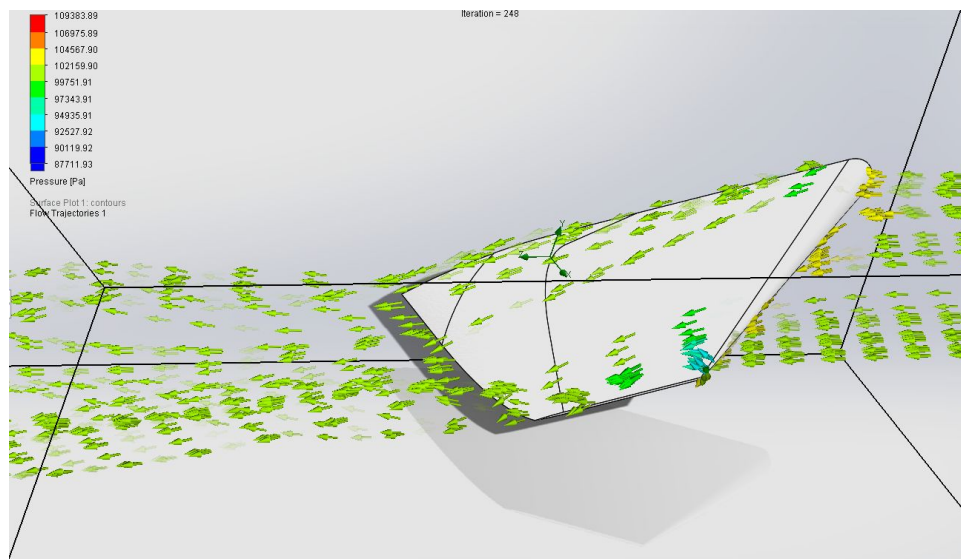

Fig 8. Solidworks flow simulation of the fin at 15AOA and 50m/s, showing laminar flow, except at the short edge, where some turbulence is observed from the curl of the velocity vector arrows. The color bar shows the magnitude of aerodynamic pressure.

Rounding the leading edges and tapering the trailing edges allows the fin to incorporate airfoil elements that smooth airflow and increases the canard's stall angle. With the changes seen in Figure 9, no flow detachment can be seen in the simulation (Figure 8) up to 15° angle of attack. Which is a safe margin to work with as the upper limit of our operational AOA is only intended to be ±10°.
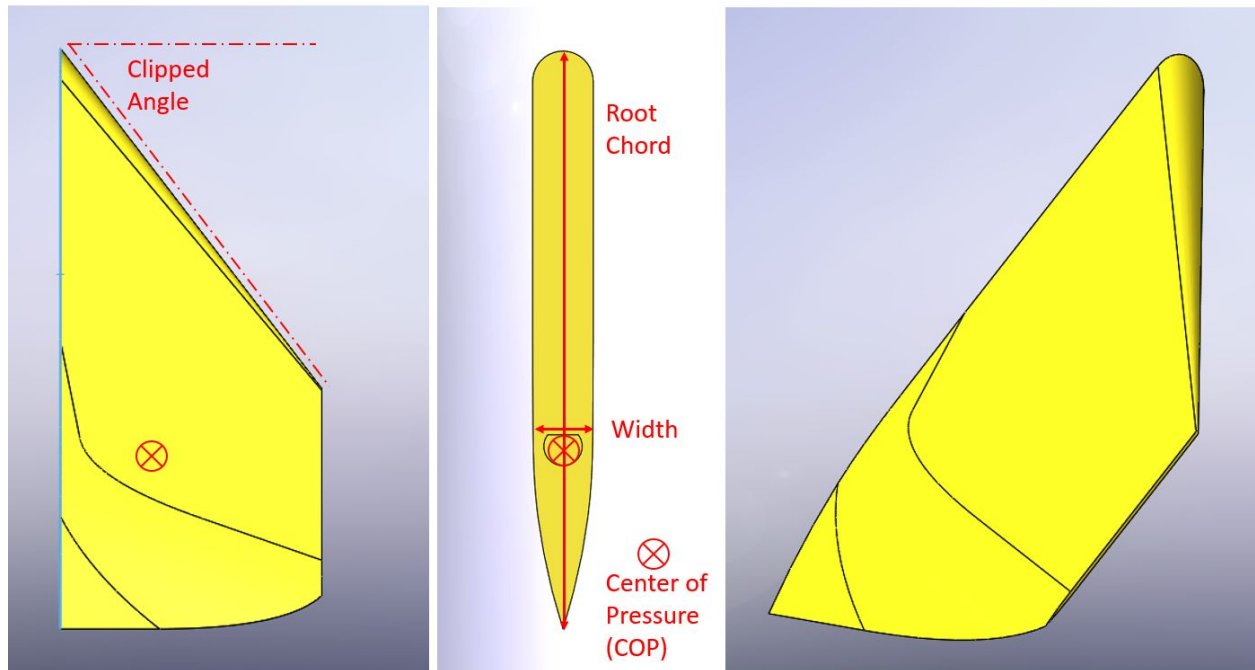

Fig 9. The final fin design captured from (left) the front view, (middle) the left view and (right) isometric view to illustrate the two axis of taper (longitudinal and lateral)

Table 4: Canard parameters from Figure 9.

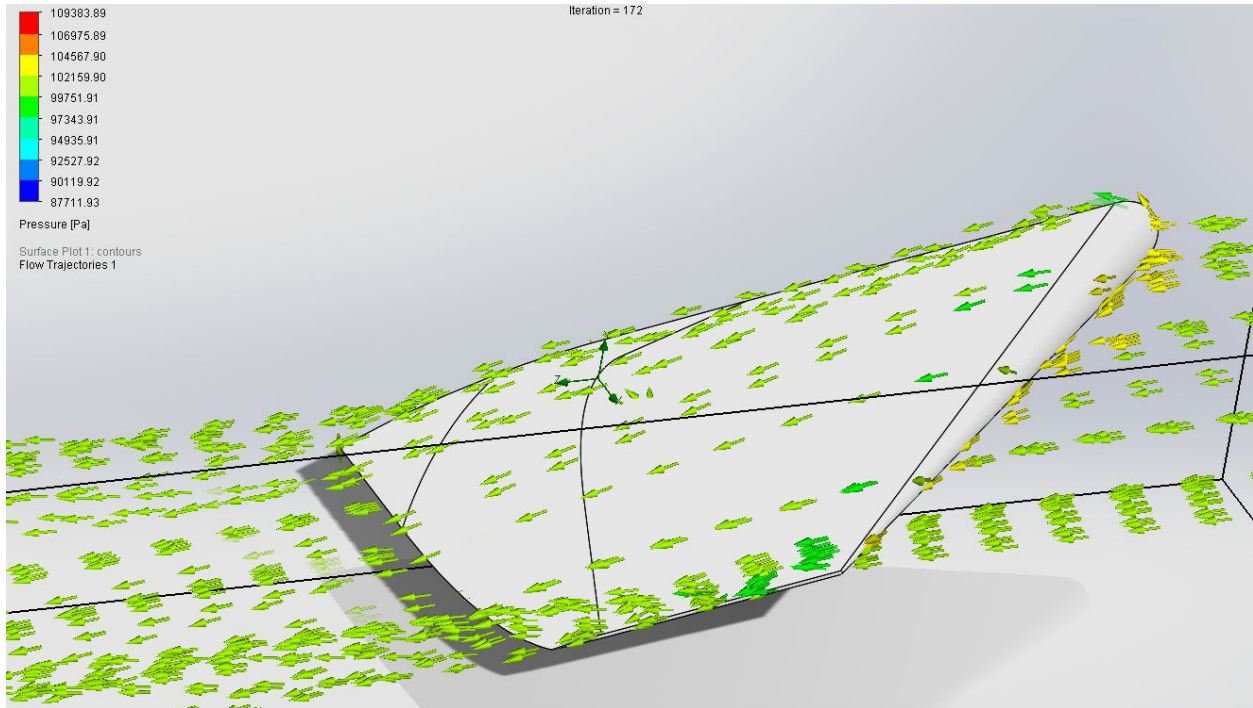| Canard Fin Parameters		
Parameter	**Unit**	**Value**
Root Chord	mm	90
Width	mm	10
Clipped Angle	°	50
Center of Pressure Position (distance into fin from flat surface)	mm	12.9
Projected Surface Area	mm^2	2723.99

Fig 10. Solidworks flow simulation of the fin at 10AOA and 50m/s, showing laminar flow, except at the short edge, where some turbulence is observed from the curl of the velocity vector arrows. The color bar shows the magnitude of aerodynamic pressure.

Table 5: Expected forces from Figure 10 simulation

Solidworks Simulation: Canard Fin at AOA=10º Airspeed = 50 m/s		
Goal Name	**Unit**	**Value**
GG Normal Force 1	[N]	0.749980133
GG Normal Force (X) 1	[N]	-0.06068052
GG Normal Force (Y) 1	[N]	**0.725978278**
GG Normal Force (Z) 1	[N]	0.178167375

Hence, to achieve the torque necessary with two fins, the moment arm from the center of pressure of the fin to the longitudinal axis of the rocket needs to be at least 29.1 mm which is within the boundary envelope of the rocket body. The edge of the canard has been placed 10mm from the body of the rocket for full assembly simulations. As seen in Figure 10, disturbances in the air flow caused by the canards appear to dissipate before the air flow reaches the tail fins. Testing in a larger windtunnel will be required to detect potential downstream effects.

The distance from the edge of the canard to the external envelope of the rocket body should be further refined and determined from simulation as boundary layers and turbulence that develop between the fin and the side of the body may cause detrimental downstream effects along the body of the rocket.
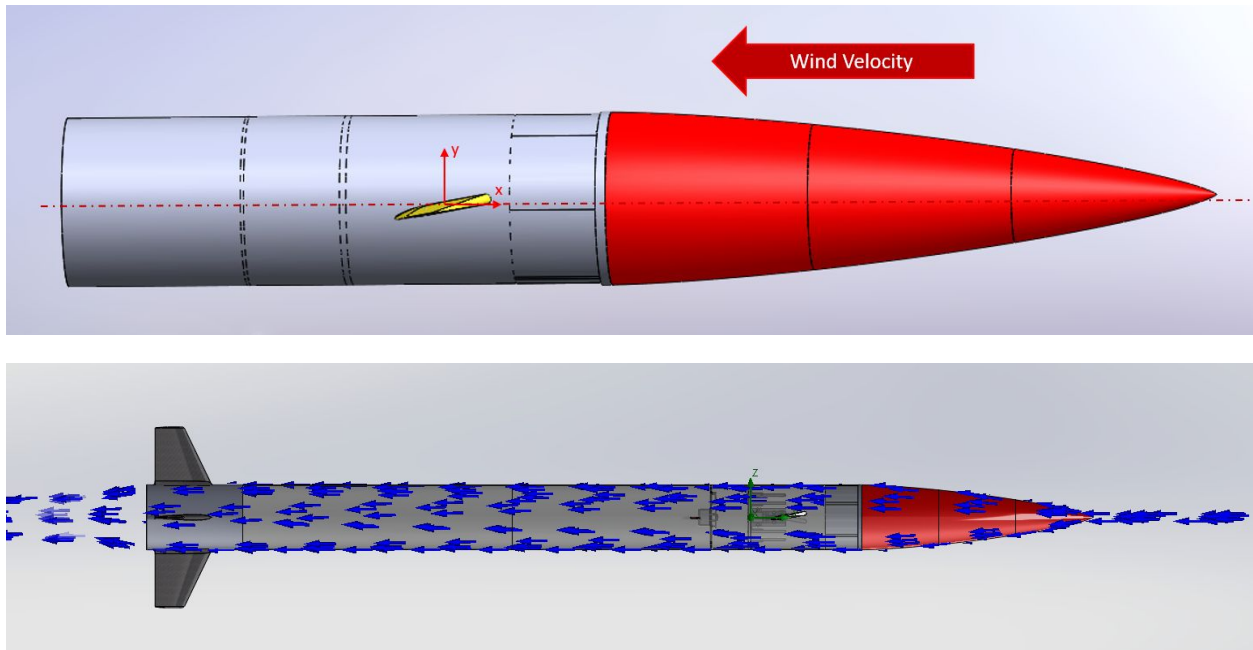

Fig 11. (top) This illustrates the wind direction during flight, as well as the X,Y axis we are referring to, in the context of the rocket body in the above table.

Fig 12. (bottom) A simple flow simulation shows that the flow is laminar throughout the entire rocket body when the canard is positioned at 10° AOA and 90 m/s. No significant turbulence is observed.
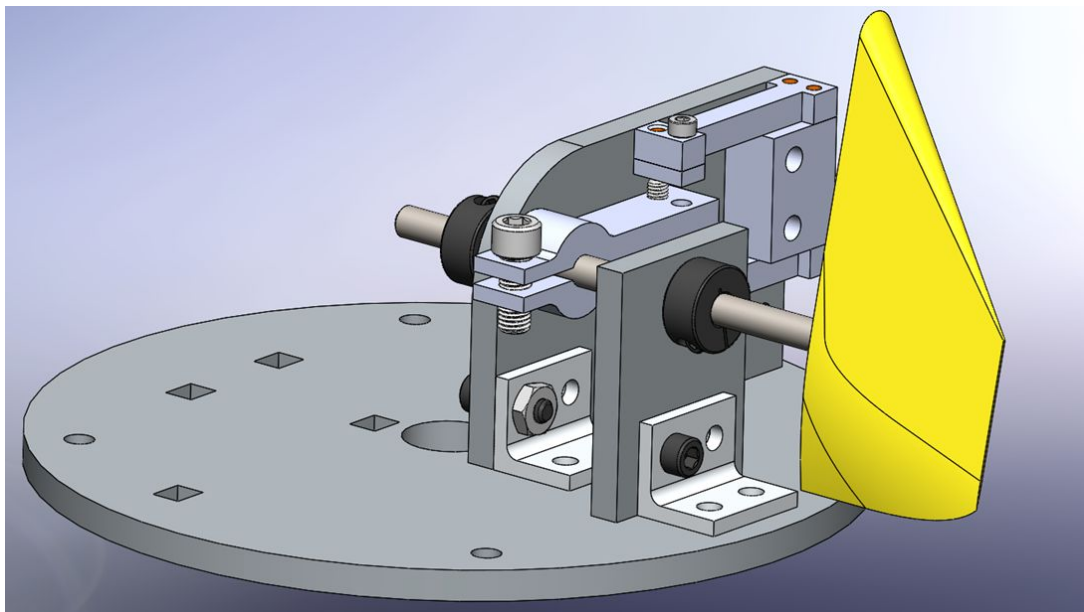
First Prototype

Fig 13. Assembly of one canard mounting mechanism in Solidworks, in isometric view

This was our first iteration and due to the large size of the standing plate, this design only allowed two fins to be mounted on the same plate. There is a center hole to allow for wires to pass through. The "arm" mounted on the shaft transfers the rotations from the fin into force input to the two load cells. Two load cells are used to measure the aerodynamic loading on each fin as the fin will experience flutter and hence will move both clockwise and counterclockwise during the wind tunnel test.
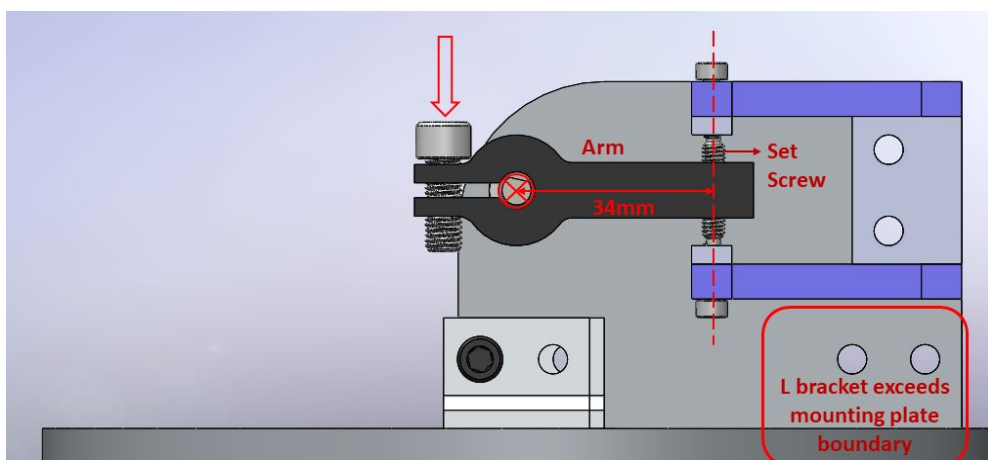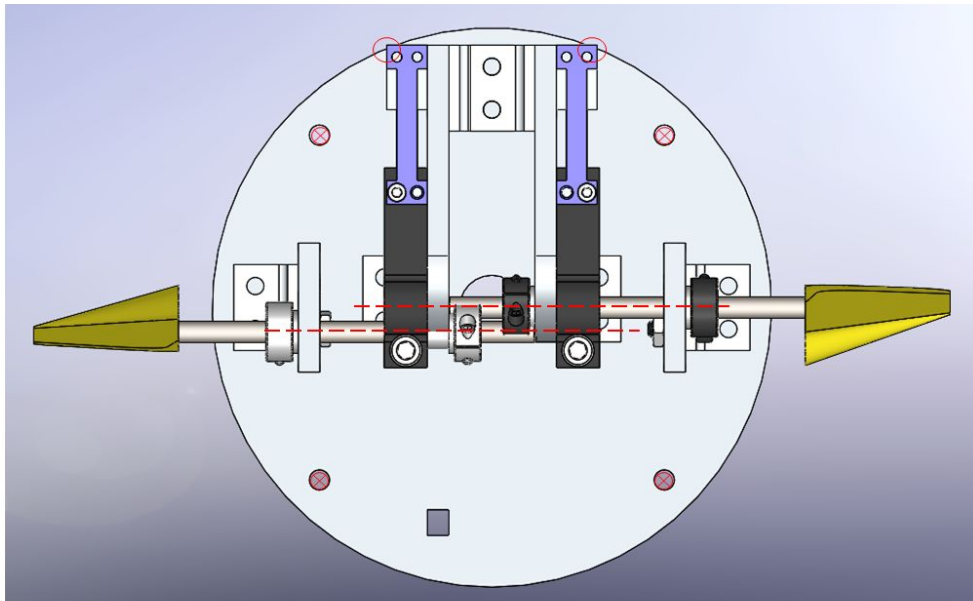

Fig 14. Front view of the assembly , illustrating important mechanisms and dimensions. The red border box shows one of the problems of this design. In situ adjustment is achieved by accessing the locking screw in the direction of the red arrow.

From Solidworks simulations, the expected lift force expected in the Y axis at 10° AOA (angle of attack) and 100m/s airspeed is 2.984N and the expected torque about the X axis is 0.0928Nm. The torque on the shaft is 0.0928 Nm and with a moment arm of 34mm (iteratively chosen between preliminary calculations and CAD drawings), the force on the load cells will be approximately 2.73 N (or 278.3 g), which is in within the range of the chosen load cell (see Table 6: TAL 221, 500g rated capacity).


Fig 15. Top view of the assembly, illustrating problems with this design.
The offset between the two shafts is undesirable and produces unintended asymmetry.

There are some design flaws in the first pass prototype.
1. There were parts that exceeded the boundary of the mounting plate.\
    a. The ends of the load cells interfered with the rocket airframe skin.
    b. Only after fabrication did we find the edge of the L bracket was outside the edge of the mounting plate.
2. The placement of the canard fins are not symmetrical about the rocket body, hence the data collected will not be accurate for the eventual intended design of symmetrical fins.
3. The set screws intended to transfer load from the arm to the load cells are difficult to access and pre-tensioning the set screws becomes a time intensive task.

Second Prototype
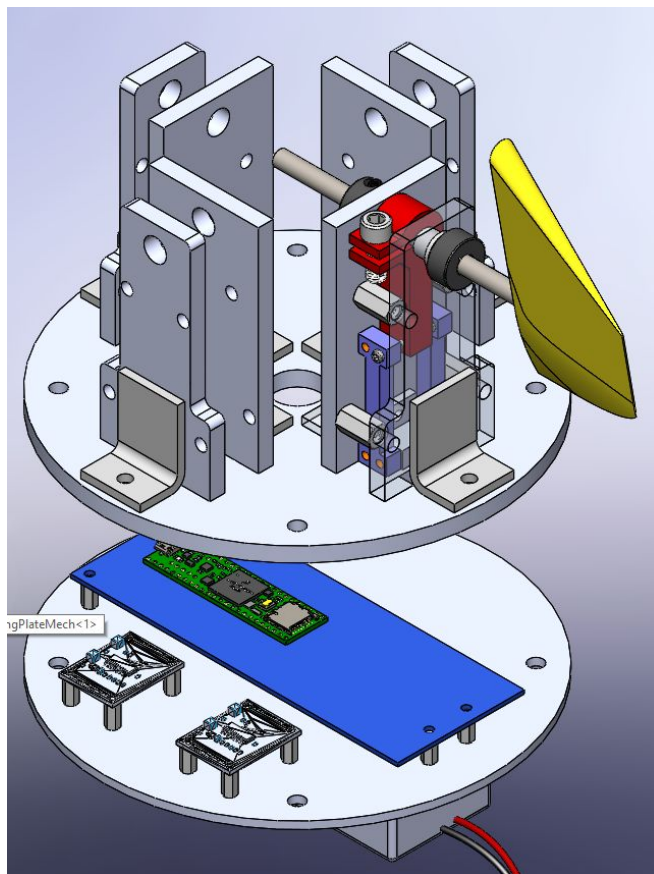
This is the second iteration of our design. This design is much more compact, allowing us to future proof for mounting four canard fins in an elegant, symmetric way within the boundary of the rocket airframe.

The total number of components have been reduced and the number of machined elements have also decreased without sacrificing precision, by making effective use of the waterjet cutter. Aside from the aluminum block that holds the two load cells which requires custom machining, every other machining operation is simple like threading or deburring.

Fig 16. The mechanical and electrical mounting plates and assemblies are shown in isometric view. The front plate of one of the assemblies is transparent to show the hidden mechanism.

34mm

The stands extend into slots cut into the mounting plate
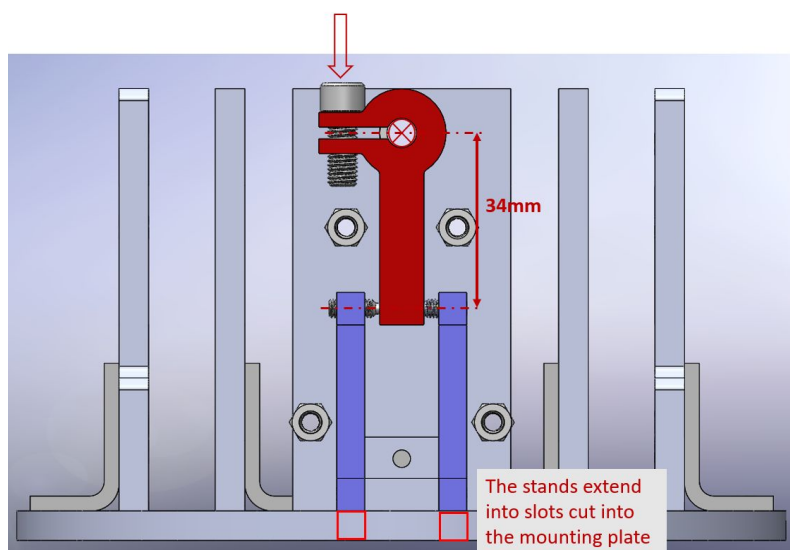
The *top* plate mounts all the mechanical components and load cells. The *bottom* plate mounts all the electronics and the battery pack is connected on the bottom face of the electrical plate.

Fig 17. (left) shows the front view of the assembly (the front mounting plate is hidden) Important dimensions and features are shown here.

17

The front and back stands have extensions that fit tightly into waterjet cut slots in the mounting plate. This helps to accurately constrain the plates' position without relying on manual machining. The arm was modified from the first iteration but still keeping in mind the necessity for easy accessibility when adjusting the canard fin.
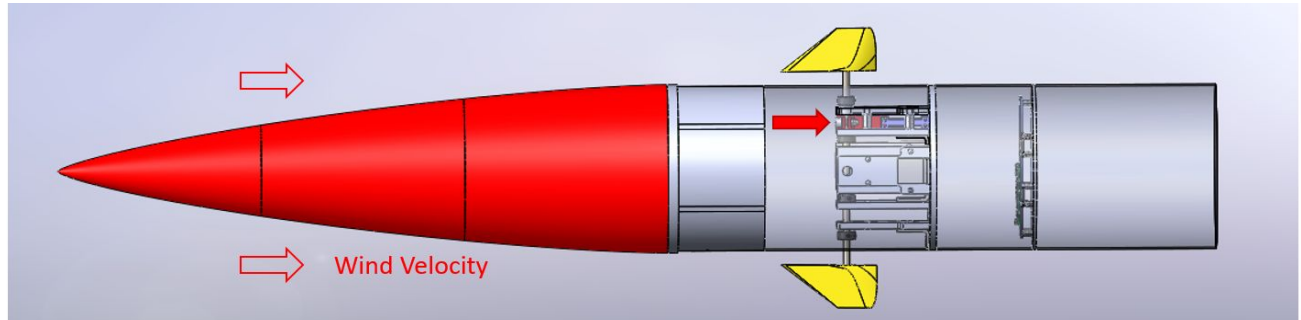

Fig 18. Shows the assemblies mounted in the rocket upper body tube. The red filled in arrow shows the direction of access to the adjustment locking screw. The angle of attack of the fin relative to the wind velocity can be changed easily this way.

The side view of the assembly shows the different methods of constraining in the assembly. The locking screw constrains the shaft rotationally. The shaft collars axially constrain the shaft and can be used to adjust the distance of the fin's center of pressure to the center axis of the rocket. The standoffs position two parallel planes an accurate distance apart and increases the stiffness of the mounting structure to resist bending and torsional loads due to the aerodynamic effects on the fin. This is important as the fin is intended to be fully constrained save for rotation about the center axis of the shaft such that all the aerodynamic forces generated by the fin can be accurately transferred to the load cells with minimal losses.
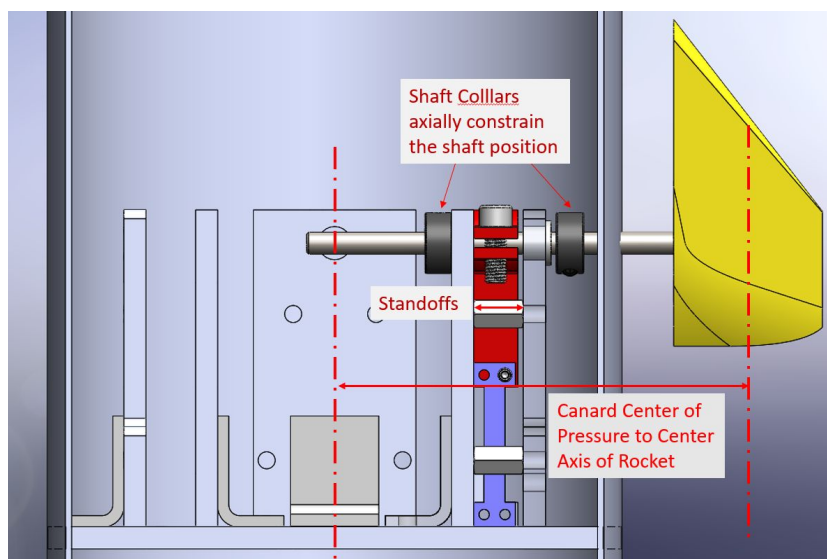

Fig 19. (left) The side view of the structure while in the rocket body tube. Important constraining features and moment arm dimensions are illustrated.

The canard center of pressure to the center axis of the rocket is 0.11845m when the flat side of the canard is 10mm away from the rocket. This has been determined to be the optimal moment arm for the canard.
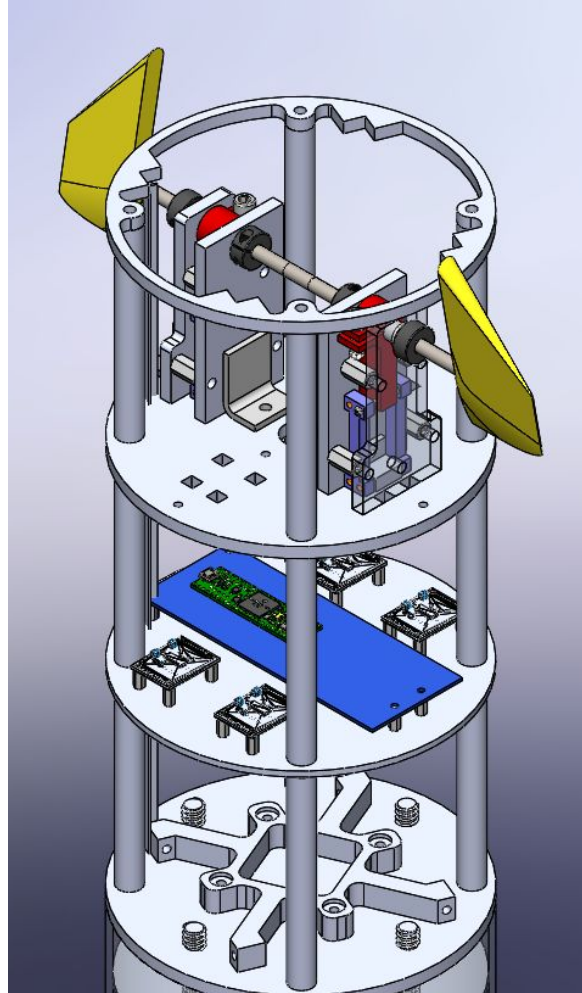

Fig 20. (left) This is the integrated internal assembly. The existing threaded aluminum rods that act as standoffs in the assembly are bolted into the holes on the mounting plate. The shaft with the canard fin has to be pushed into the mounting plates after the carbon fiber airframe is slid over the internal assembly, but does not have to be removed at any point during the wind tunnel test.
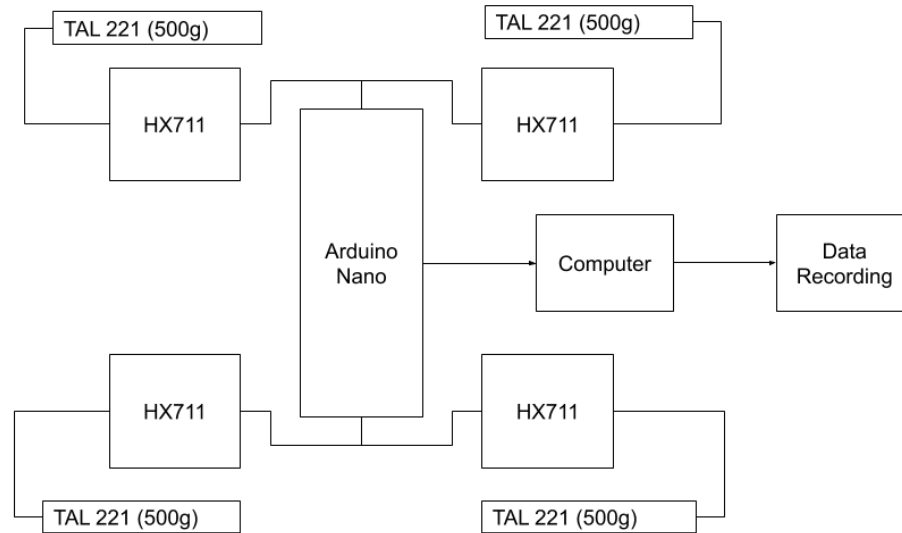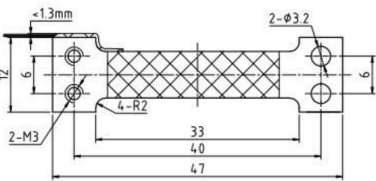
Electrical Design

Fig21. Schematic for Electrical System for Static Module

Table 6: Electrical Component list and key specifications

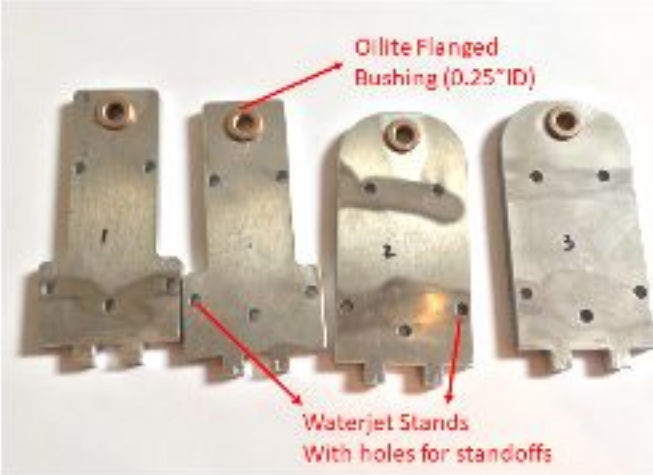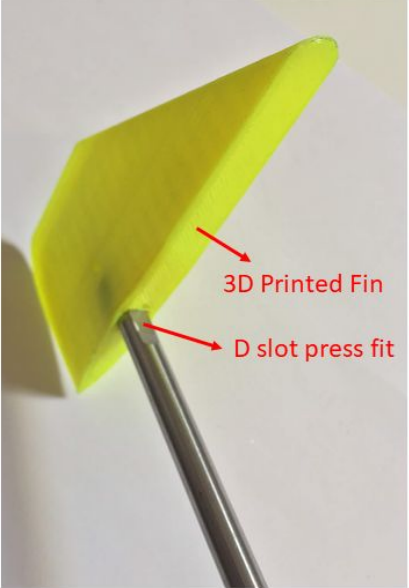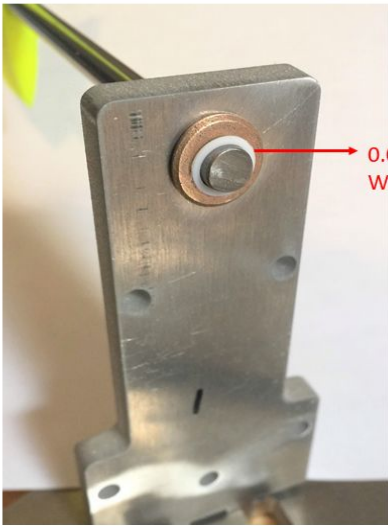| Component Chosen	Relevant Specifications
Load Cell - TAL 221 (500g Load Capacity) *Fig 22. Engineering drawing of load cell. Obtained from the TAL 221 datasheet on sparkfun.com*	Rated Output: 500g Ultimate Overload: 200% of Load Capacity ● 500g gives us a safety factor of about 2.5 with respect to expected aerodynamic loading of 198g. Hysteresis: 0.05% of Load Capacity ● Low hysteresis allows us to conduct multiple consecutive tests with minimal calibration needed. Operating Temperature: -10°C - + 40°C There are many form factors of load cells. We chose a single point beam type load cell as the compact packaging was ideal and there was a model in the 500g load capacity range.
Load Cell Amplifier - HX711	Analog to Digital Conversion with 24 bit accuracy. ● 24 bit is on the order of 10^7 magnitude, which will

	theoretically give us a precision of 50 micrograms. (In reality, there will be a healthy amount of noise that will reduce the effective precision) Gain can be set to 128, 64 or 32. When using an external clock, we can obtain 80 samples per second (SPS). The minimum settling time for a stable output is 40ms, so theoretically the maximum sample rate could be 200Hz.
Microcontroller - Arduino Nano Atmega 328p Microprocessor	Clock Speed: 16 MHz ● To get one reading from the amplifier, the clock needs to pulse 24 times, which only uses 1.5 microsecond. The processing power is much more than what we need for this application. Operating Voltage is 5V, which is between 2.6V-5.5V necessary for logic operations when interfacing with the amplifier. 16kB flash memory for storing code USB port can draw up to 500 mA @ 5V ● Current for each HX711 board = 0.1mA ● Current to power Arduino Nano = 19mA ● Hence the USB port is enough to power the static module.

Tests & Discussion

Mechanical Fit Assembly

For the master parts list, please refer to Appendix C.

Table 7: Mechanical Assembly guidelines

Fig 23. Four waterjetted stands for an assembly with two canards. Important features are marked out.

Holes were tapped to fit the threaded standoffs. The plates were cut from ¼" aluminum sheet to provide enough thickness for the threads and shaft support.

Oil embedded flanged bushings were press fit into the center top hole to reduce friction as the shaft rotates.

Fig 24. (left) The 3d printed fin (PLA material) was press fit and epoxied onto the D slot part of the shaft.

The shaft uses a drill rod, which is a hard material, with low tolerance and a finished surface.

Fig 25. Closeup of where the PTFE washer sits. It contacts the rotating arm to provide a surface with low friction
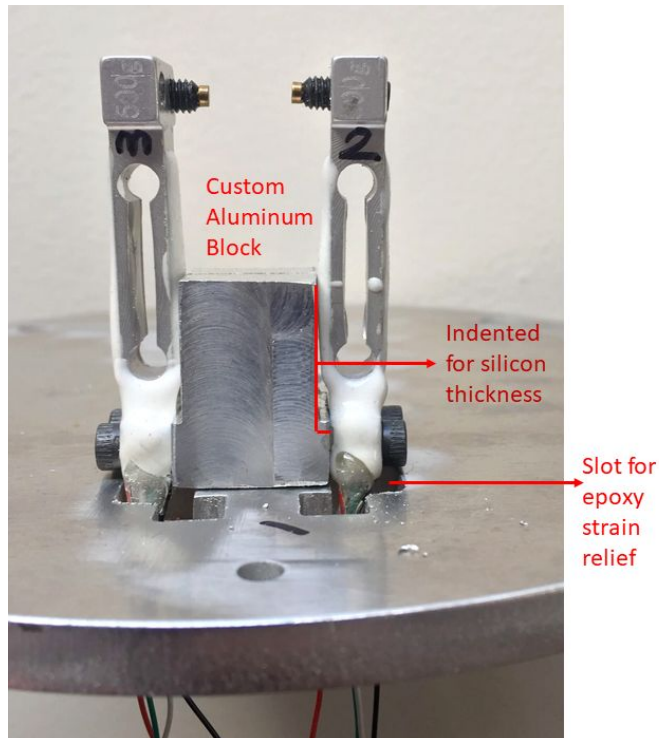
Fig 26. The aluminum block holding the two load cells is a custom machined piece and is bolted down to the mounting plate. It sits between the front and back mounting stands.
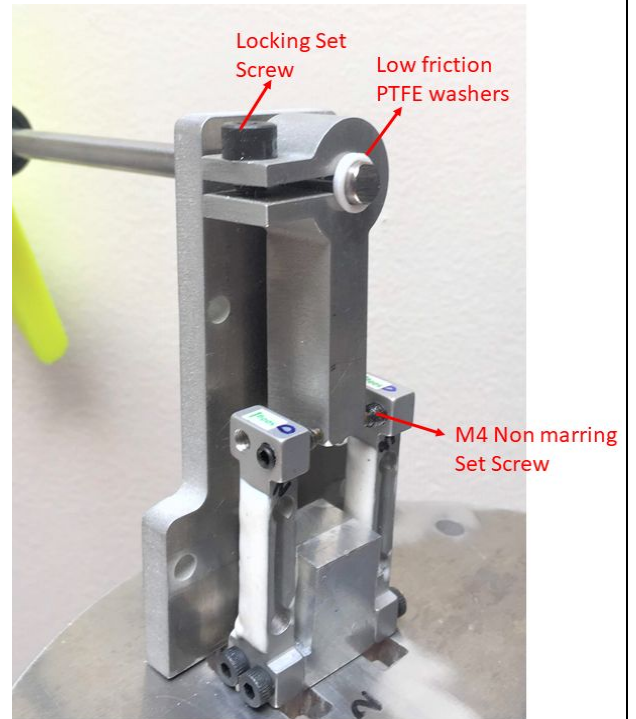

Fig 27.The "arm" on the shaft uses the locking set screw to tightly clamp onto the shaft and effectively transfers any movement from the fin to the load cells. The non-marring set screws are pre-tensioned on each side of the arm. There are PTFE washers on each side of the arm to reduce friction from surface contact.

Overall, the parts fit well together and were easy to assemble and put together. Minimal machining needed to be done as most parts were waterjet cut then fit together. The design for the Dynamic Module can be based off of this design with little modifications needed to mount the servo actuation.

Electrical Testing

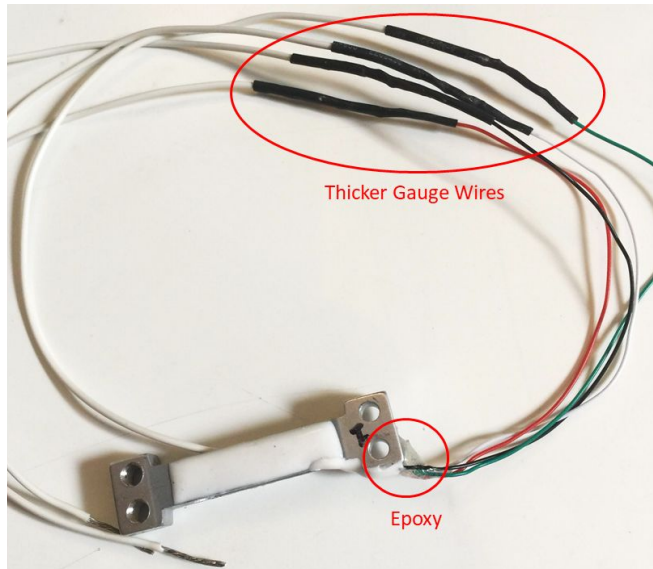We are using the TAL 221 load cell with a load capacity of 500g.

Fig 28. (left) The load cell chosen comes with fine wires so we experienced some wire breakage initially when trying to modify the mounting holes in the load cell. The picture on the left shows modifications we made to each load cell.

We found that some epoxy as additional strain relief (manufacturer's silicone layer was not strong enough) and soldering on #22 gauge stranded wires allowed easy handling and testing of the load cell.

Characterization of Load Cells and Amplifiers

We tested 6 load cells in total, numbered #0, #1, .. , #5 and Amplifiers #0, .., #3. Due to the constrained circumstances that we were conducting this test, proper weights were not available. Instead the load cells themselves were used as test weights as their weight is within the load capacity and are assumed to have relatively low variation between load cells.
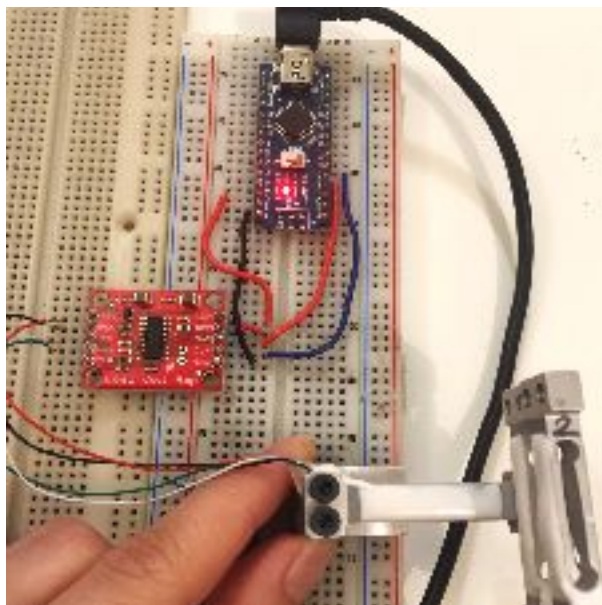
The load cells were tested using the same HX711 Load Cell Amplifier and using the same test procedure described below. The setup used an Arduino Nano with an Atmega 328P microprocessor.

Fig 29. (left) TAL221 bench testing setup with HX711 Amplifier and Arduino Nano. This also shows two load cells stacked on top of the load cell under test, acting as near identical test weights.
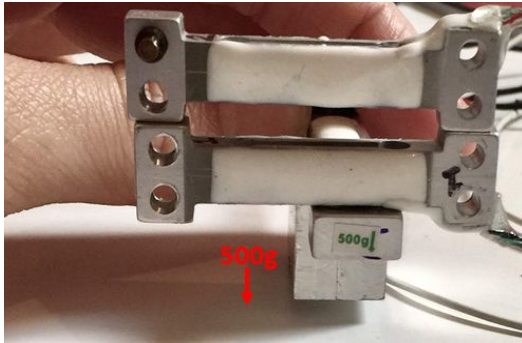
Fig 30. (left) Shows the stackup of the "test weights". The weight is applied in the direction suggested by the manufacturer.

Test Procedure:

- Connect the load cells to HX711
- Bolt the load cell onto aluminum block and hold it steady on a table during test
- Orient in the "down" direction as indicated by manufacturer's sticker
- Around 3 seconds, place one load cell as weight at the far end.
- Around 8 seconds, place second load cell on top of the first, also at the far end
- Around 15 seconds, take off both weights at the same time
- At 20 seconds, the test will stop
- Data is recorded off the serial monitor. Repeat for load cells #0 - #5

* Individual Load Cell and Amplifier testing results are in Appendix B

** #1, #3 load cells are omitted from the following graphs as they were not operational at the time of testing.
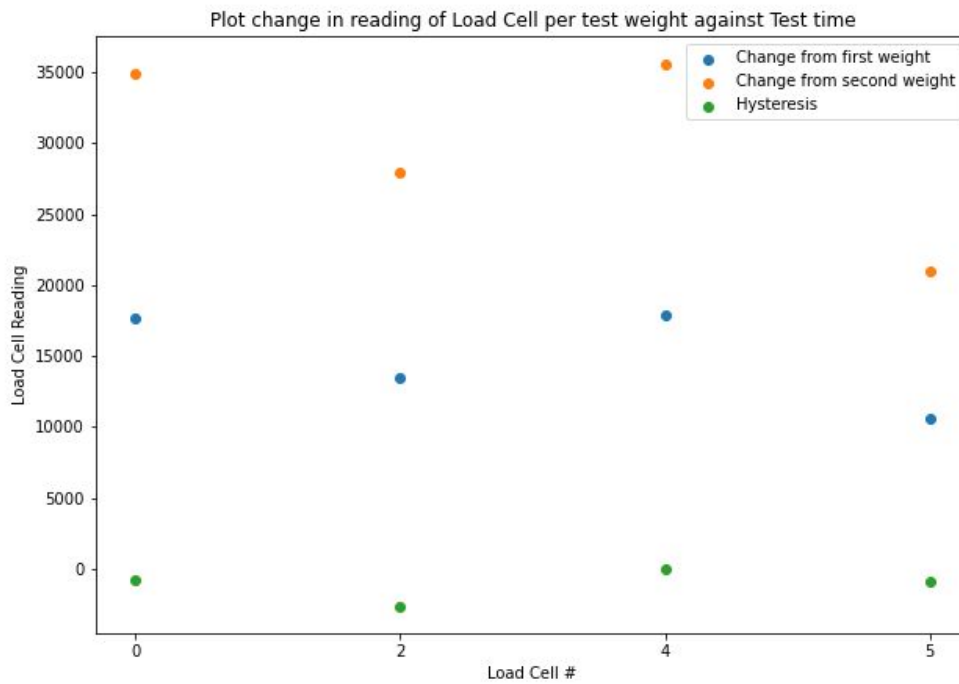
Fig 31. Graph of all four load cells and their change in readings for the first weight, the second weight, and from the initial zero reading (hysteresis). Plotted using the matplotlib library in Python.

Table 8: Load Cell measurement Precision results

	Average Δ Reading	Average % Error
First Weight	+14898.75	19.4%
First + Second Weight	+29879.50	18.1%
Hysteresis (Final Reading - Initial)	1063.75	0.707%

The first and second weight have an average change in reading of 14939.75 with a deviation of only 1.0% across all four load cells. Hence, we can conclude that these load cells behave linearly within the rated capacity and produce repeatable, accurate measurements.

For testing of the HX711 amplifiers, the same test procedure was used, exchanging out the amplifiers (#0 - #3) instead of the load cells. A single load cell with the most stable reading was chosen. That load cell is #2.
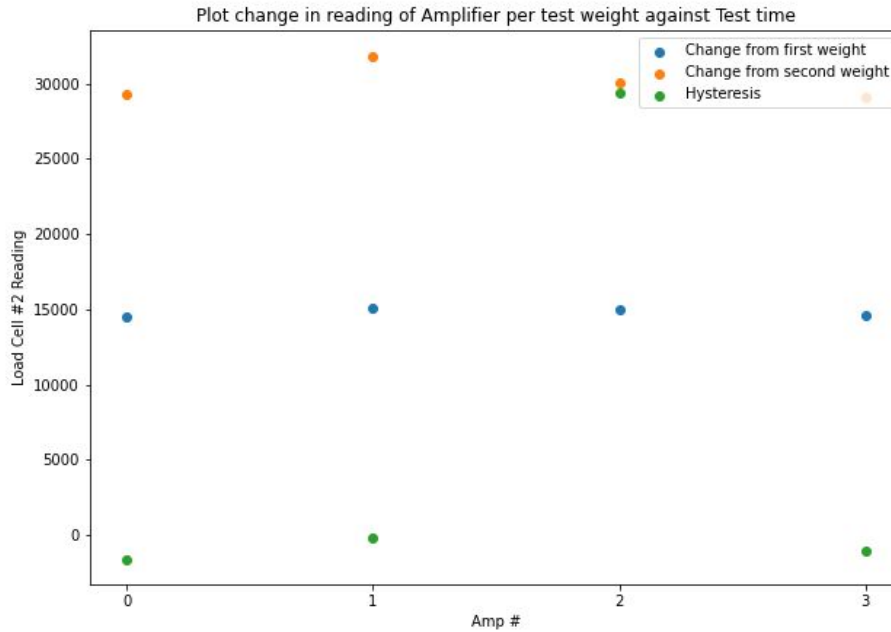
26

Fig 32. Graph of all four amplifiers and their change in readings for the first weight, the second weight, and from the initial zero reading (hysteresis). Plotted using the matplotlib library in Python.

Table 9: Load cell post amplifier measurement precision results

	Average Δ Reading	Average % Error
First Weight	+14781.25	1.57%
First + Second Weight	+30060.75	2.95%
Hysteresis (Final Reading - Initial)	8053	2.81%

The high % error between the load cells in detecting the test weights should be further investigated. The TAL 221 datasheet shows that we should expect a hysteresis error of 0.1%, while our rudimentary test shows 0.7%. The test method used has inherent errors as the test weights could be skewed while placing and the load cell may not be level. The load capacity up to 500g should also be tested and verified.

The amplifiers seem to deviate very little when tested on the same load cell. Strangely enough, the hysteresis is higher than the load cells but with a low error of 2.81%, this should not significantly affect the accuracy of the readings.

27

The tests show the necessity of calibration. As the load cells are very sensitive (slight shaking or shifting of the test weight produces distinct bumps), the calibration will be setup dependent and so it should be done in a nearly identical orientation outside the wind tunnel. A zero calibration needs to be done before every test as the zero point reading differs more than +/- 100000 counts between tests.

Wind Tunnel & Aerodynamic Simulation

Unfortunately, we were not able to test the system we built even though we managed to book the wind tunnel at UBC. Instead we will be using simulation to supplement the lack of wind tunnel data. The moment arm used is 0.119m. The rows highlighted in green represent the torque produced by the canard is higher than the minimum requirement of 0.140Nm.

Table 10: Canard Loads vs Airspeed at 10° Angle of Attack

10° AOA			
Airspeed (m/s)	Force in y direction (N)	Torque per Canard about rocket (Nm)	Torque about Shaft (x-hat) (Nm)
10	0.034723063	0.003661547	0.000839701
20	0.137946391	0.014546447	0.003400818
30	0.301764638	0.031821081	0.00779936
40	0.5078211	0.053549735	0.014275205
50	0.725978278	0.076554409	0.023212377
60	1.032495509	0.108876651	0.033674966
70	1.417383378	0.149463077	0.045770199
80	1.873173664	0.197526163	0.059521073
90	2.406720956	0.253788725	0.075077758
100	2.984071201	0.314670308	0.092835138

Table 11: Canard Loads vs Airspeed at 5° Angle of Attack

| 5° AOA			
Airspeed (m/s)	Force in y direction (N)	Torque per Canard about rocket (Nm)	Torque about Shaft (x-hat) (Nm)
10	0.015866371	0.001673109	0.000414137
20	0.062419503	0.006582137	0.001694515
30	0.13231795	0.013952928	0.003932824
40	0.238656451	0.025166323	0.006963456
50	0.311278304	0.032824297	0.011645892
60	0.350358242	0.036945277	0.018108513
70	0.594133449	0.062651372	0.023188427
80	0.777163864	0.081951929	0.030169481
90	1.035253712	0.109167504	0.038149444
100	1.376079449	0.145107578	0.045956489
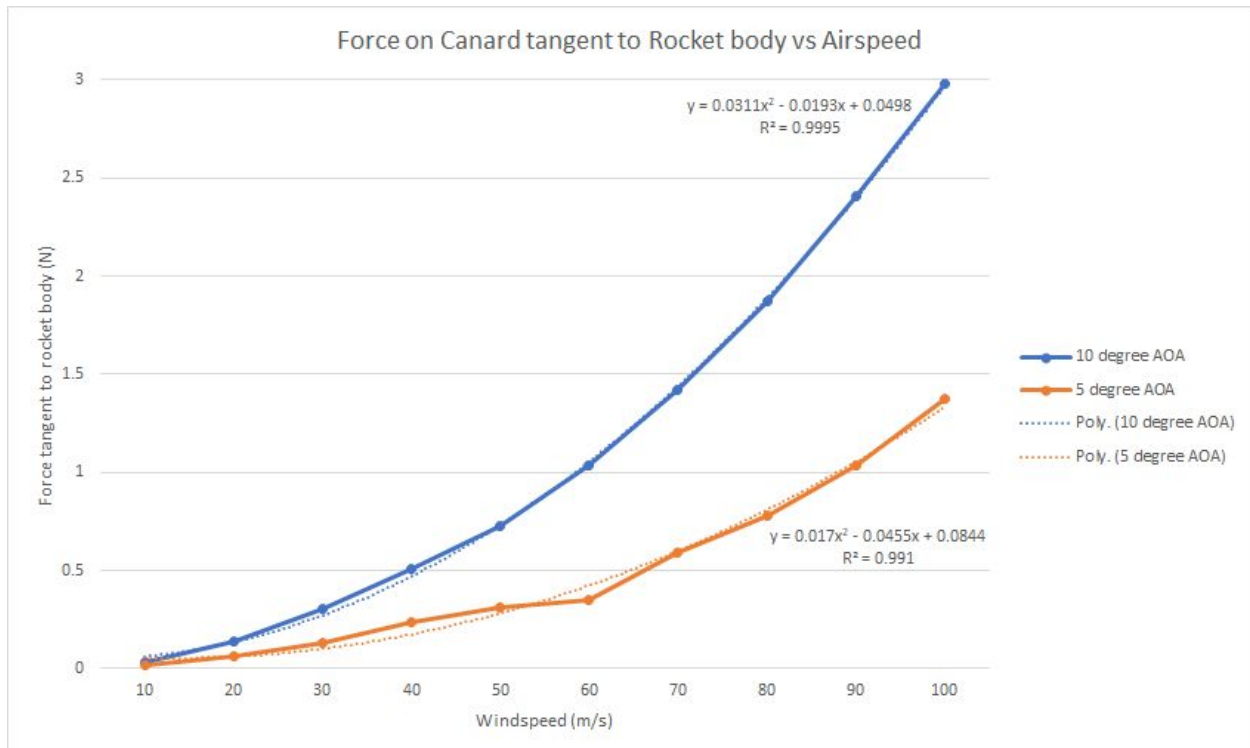
Fig 33. Plot of Lift Force versus Airspeed. At 10 degrees AOA, the increase in lifting force is nearly twice as quickly as when the canard is positioned at 5 degrees AOA. Plotted using Excel.

Fig 34. Plot of extracted lift coefficient values for 10 and 5 degrees AOA, versus airspeed. We can observe that the coefficient of lift for each AOA decreases around 50-60m/s airspeed and seems to fluctuate around 0.12 for 5° AOA and 0.25 for 10° AOA beyond 60m/s.

Using two canards this countertorque can be achieved at 10° AOA in an airstream moving relative to the rocket at speeds of at least 50m/s. At 5° AOA, the minimum airspeed necessary increases to 80m/s. From the full scale rocket simulation done by UBC Rocket, the airspeed reaches 50.920m/s at 2.23s flight time and reaches local speed of sound (Mach =1) at 13.4s.

To analytically determine the torque at Mach 0.95 (<1):

- C_L value from simulation = 0.25

- Compressibility factor = $\dfrac{1}{\sqrt{1-M^2}}$ = 3.21

- Atmospheric Pressure of 67200 Pa (when M= 0.95)

- Atmospheric Density of 0.878 kg/m^3 (when M=0.95)

- Velocity = Mach Number x Local Speed of Sound = 315.23 m/s

- Relevant Surface Area = 2723.99 mm^2

The lifting force experienced by the canard hence will be expected to be in the same magnitude as 95N and we can safely assume that the canard will be effective from about 2.23s - 13s of flight time with increasing margin.

Conclusions

Based on our simulations, the canards are theoretically able to produce more than the minimum torque requirement to effectively control the roll rate of the rocket in the subsonic region of flight. We have high confidence that canards will be able to control the rocket below the transonic region (which starts at Mach 0.8).

However, Solidworks simulations are simplistic and do not account for compressibility and transient effects at higher speeds. The transient effects of the fin deflecting quickly at high speeds need to be investigated. This could potentially produce vortices that can cause fin flutter in the tail fins to occur at lower than expected airspeeds. This is a big risk as fin flutter can potentially cause structural damage to the fin can, and irreparable damage to the rocket.

The inability to verify simulations at high airspeeds contributes to the high uncertainty in determining the behaviour of canards as it nears the transonic region. Without being able to accurately quantify when and how their behaviour deviates from expectation, control parameters will not be as reliable.

Recommendations

Currently, only the hardware for the Static Module has been completed. The immediate next steps is to assemble into the Skypilot rocket's upper body tube and conduct the wind tunnel test, as described in Appendix D. If the data is on the same magnitude as the simulation results and there is a good signal to noise ratio, then the coefficient of lift can be extrapolated for low subsonic speeds.

A valuable analysis to conduct would be to simulate the lift force generated by the canards throughout the subsonic region of the flight, which is the intended use case. The following is the environmental condition of the flight just as the rocket exits the subsonic region.

Table 12: Whistler Blackcomb flight path environmental conditions immediately before leaving subsonic region

Speed	(Local) Mach 1.02
Altitude	3.57 km
Atmospheric Pressure	65143 Pa (64% at sea level)

As the lift force is generated proportionally to the velocity squared and linearly proportional to atmospheric density, this analysis will estimate the effective region of control that the canard can exert on the rocket over the flight trajectory. The analysis should also be accompanied by a more sophisticated simulation using finer meshes and molecular interactions between air molecules as the airspeed approaches the sound barrier.

Furthermore, as conserving mass is critical in rocket design, the full scale model should be estimated in terms of the mass budget and packaging size. The servo will be the main drain of power as it needs to hold the position of the canard while resisting the aerodynamic forces, so power requirements and battery weight required should be sized as well. These parameters should be compared to other implementations for active stabilization like cold gas thrusters. This step is suggested before deciding to design and build the Dynamic Module.

Deliverables

CAD Design:
- We have a GrabCad project that has been shared with the sponsor, UBC Rocket. This project contains all the previous and current revisions of all the files.
  - GrabCAD\Canards\Static Module Feb 17 - This is the folder containing the current Static Module assembly named "StaticModuleAssem.SLDASM".
  - GrabCAD\Canards\Canards - This is the folder containing simulation files and different iterations of the canard fin.
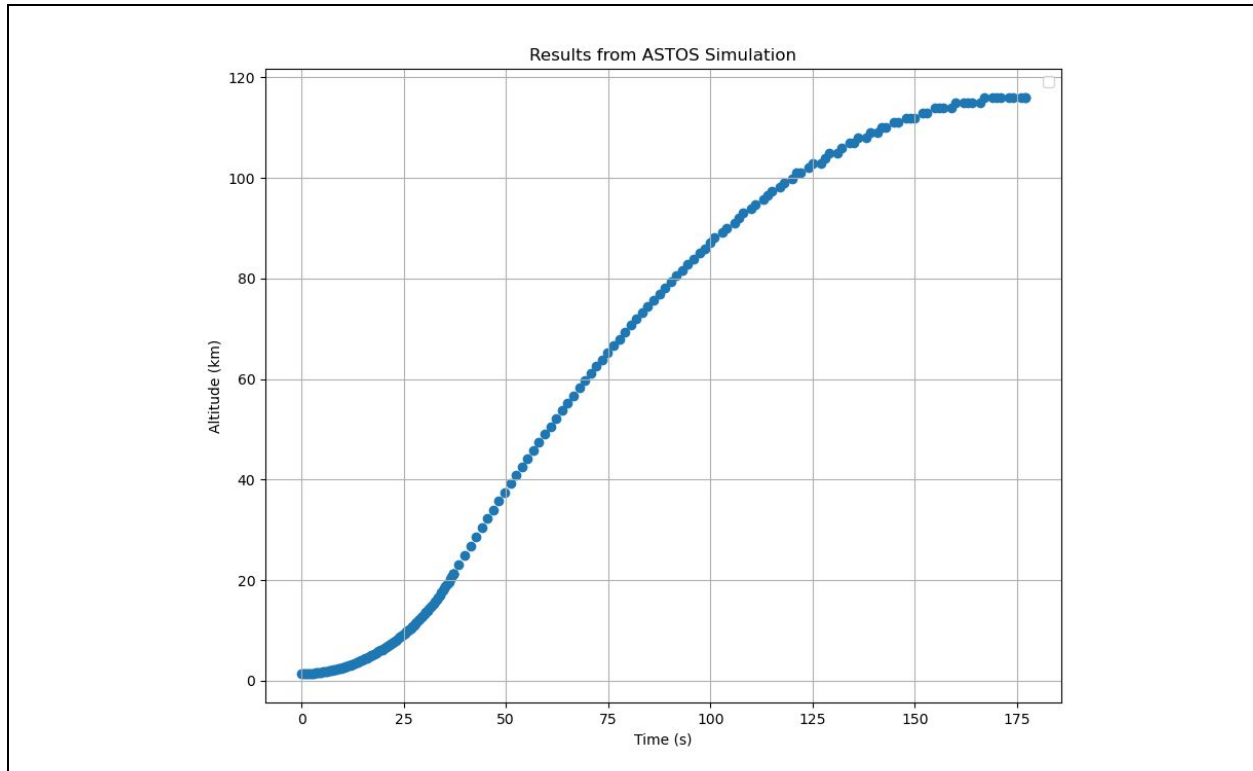
- GrabCAD\Canards\Load Cell Testing - This folder contains the data, plots and code for testing load cells and the amplifier.
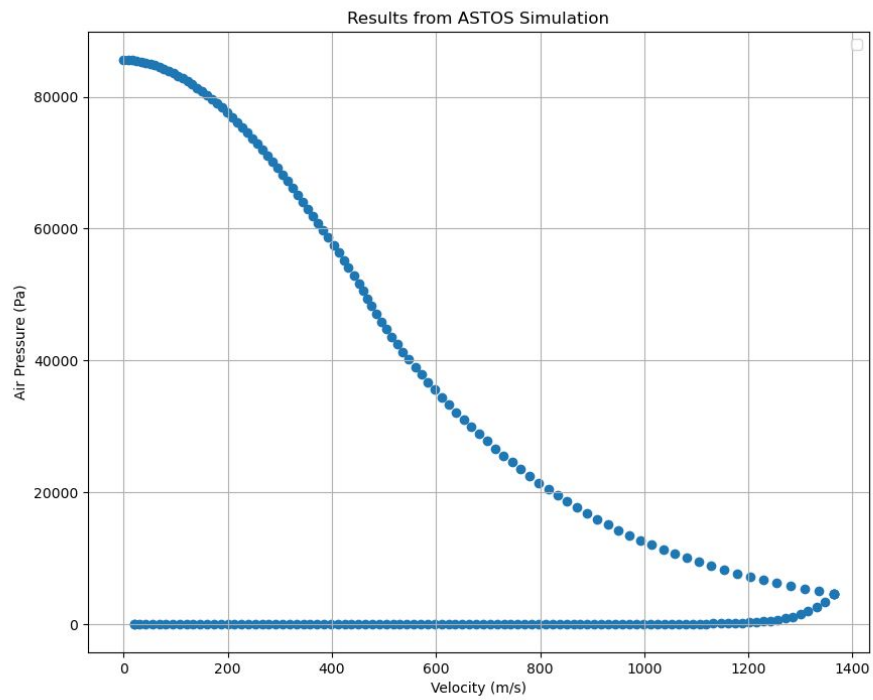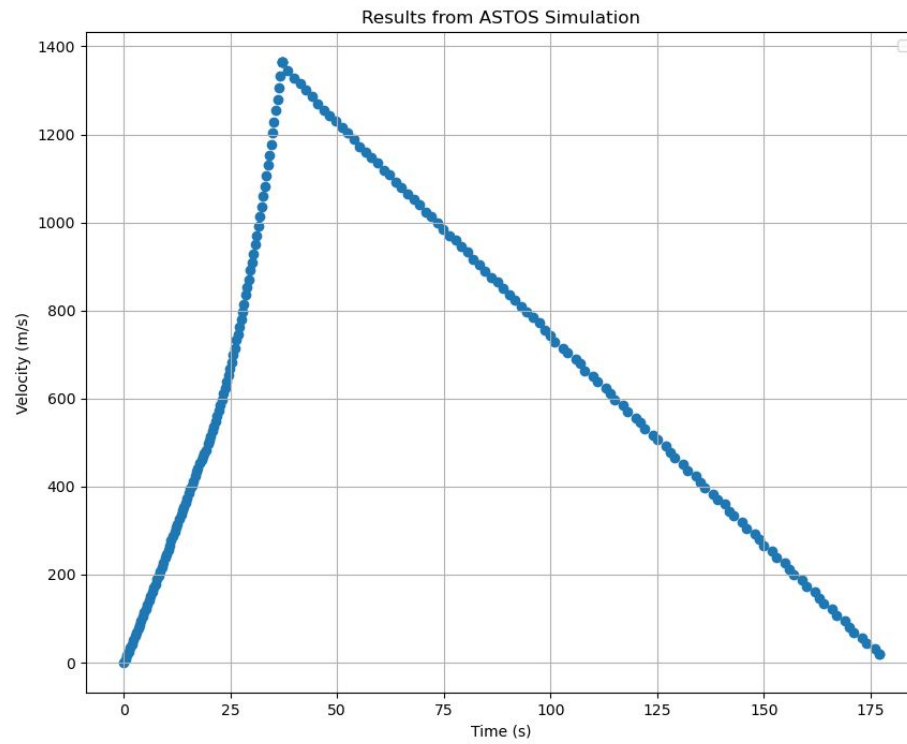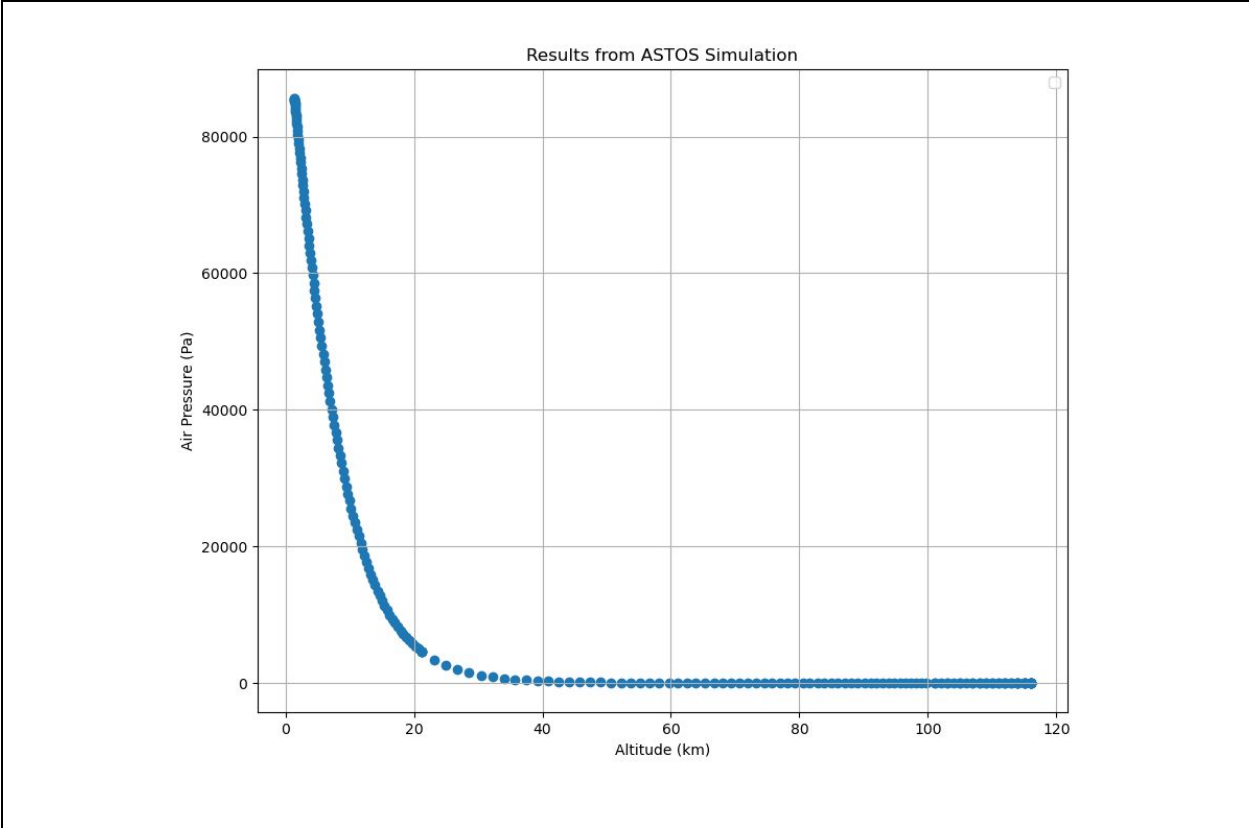
Hardware:

- Static Module Mechanical Hardware:
  - Assembled mechanical plate, with two assemblies to mount one canard fin each.
  - Each assembly consists of two stands, an arm with locking screw, two load cells bolted to the custom aluminum block, standoffs, bushings, shaft with a D slotted end and a 3d printed fin.
- Static Module Electrical Hardware:
  - Electrical components consist of four HX711 Amplifier boards and four load cells. All electrical components have been fully soldered and verified to be in working condition.
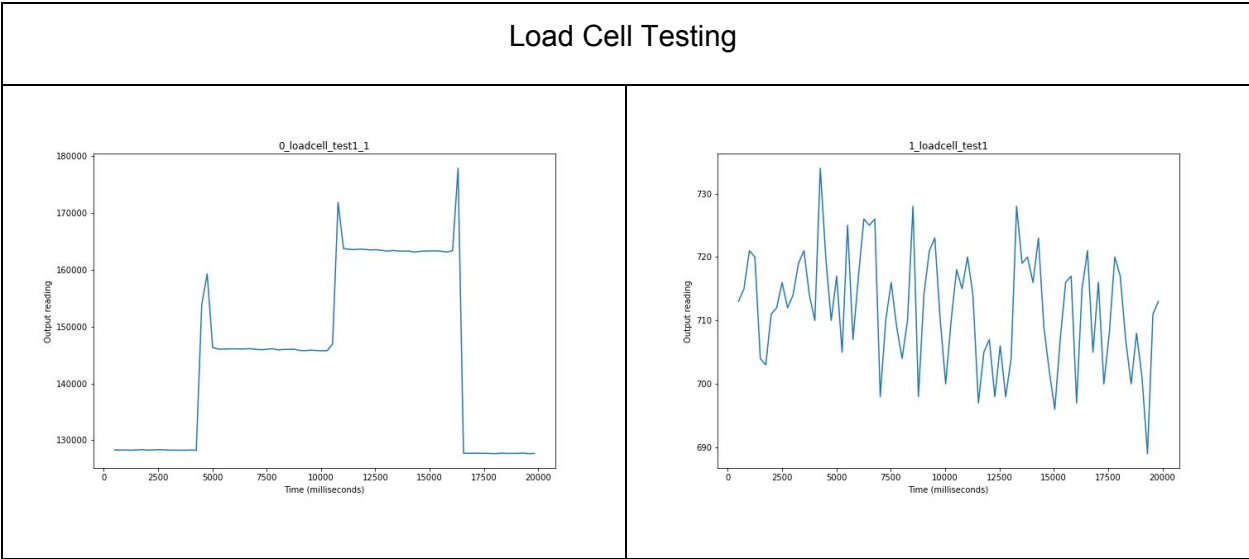 - Attachments to the electrical mounting plate with mounting plates and standoffs are installed.

Appendices

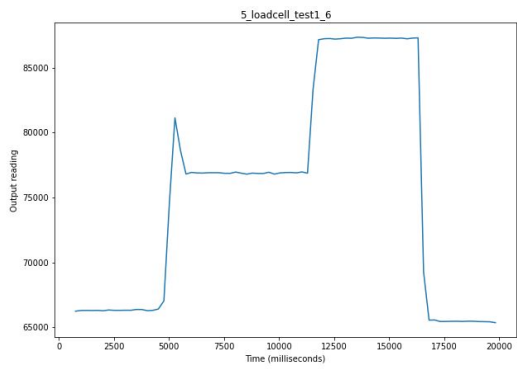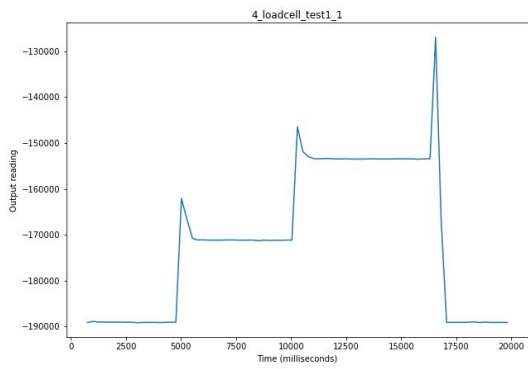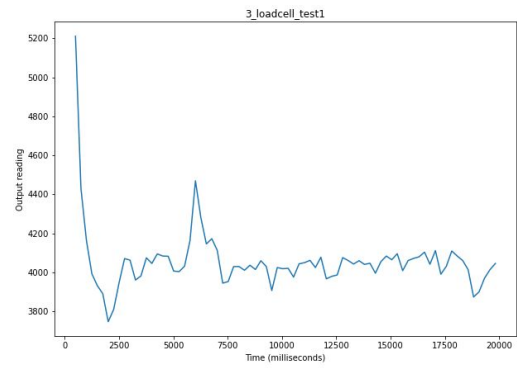## Appendix A - ASTOS Simulation for Whistler Blackcomb Rocket

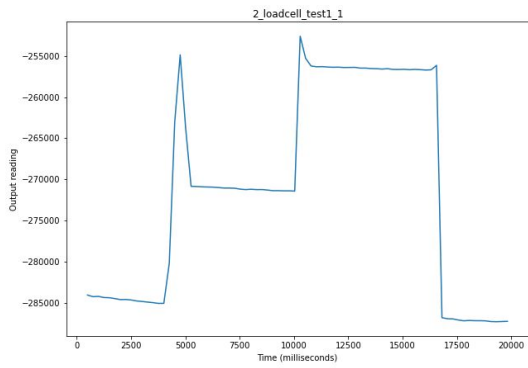Results from ASTOS Simulation

Appendix B - Results from Load Cell and Amplifier Testing

Load Cell Testing

2_loadcell_test1_1

3_loadcell_test1

4_loadcell_test1_1

5_loadcell_test1_6

Amplifier Testing

0_amp_test2

1_amp_test2
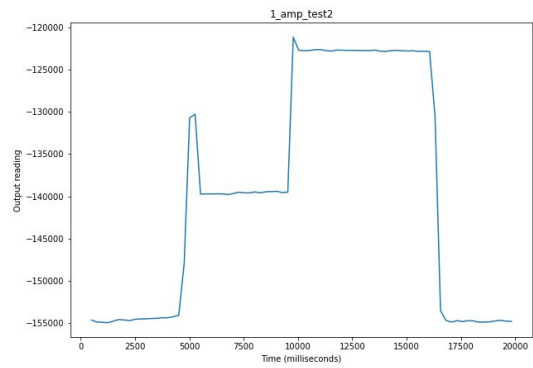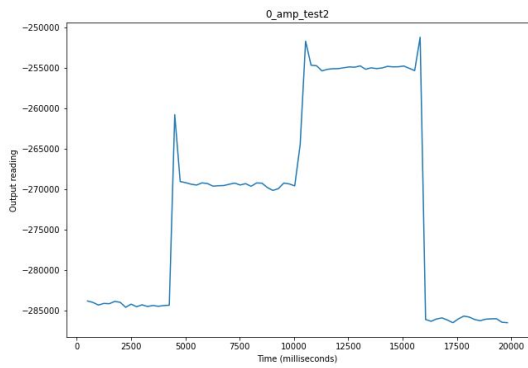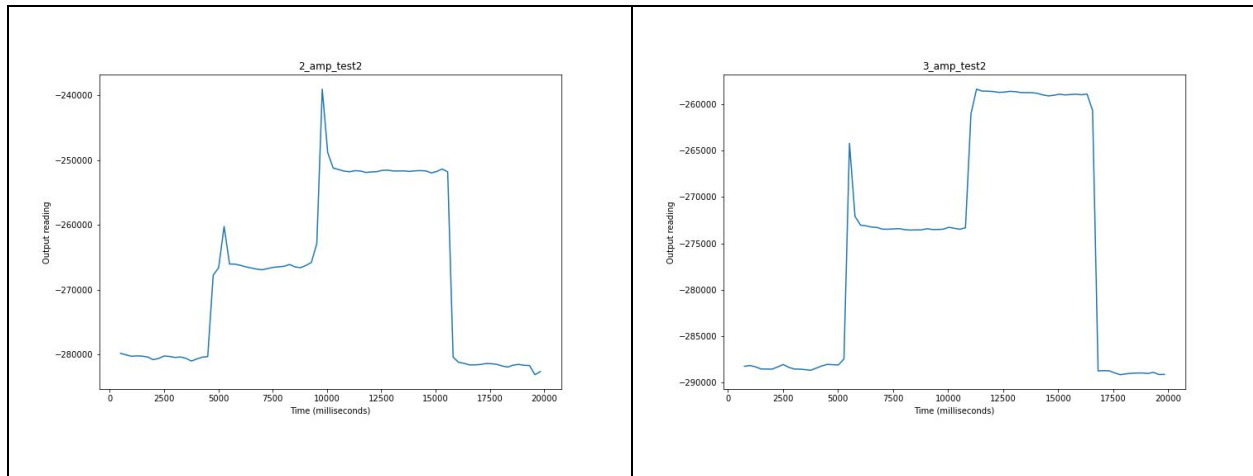
Appendix C - Master Parts List

Table 13: Mechanical Bill of Materials

Mechanical Components	
Part Description	Source
10-32 x 9/16 Length Aluminum Hex Female Standoff	91780A645 MMC
M3-0.5mm, 10mm Long standoffs	95947A006 MMC
.26" ID, 0.022"-0.028" PTFE Washer	95630A217 MMC
Steel Socket Screw M3 x 0.5mm x 10mm Long	91290A115 MMC
Clamping Shaft Collar ¼" Diameter	6435K12 MMC
0.25"ID 0.375" OD Oil-Embedded Flanged Sleeve Bearing	6338K411 MMC
10-24, ⅝" Long Socket Head Screw	91251A244 MMC
M4-0.7m Metric Alloy Steel Brass Tip Set Screw	94085A114 MMC
M3 x 0.5 mm Thread, 10 mm Long	91290A115 MMC
Button Head Hex Drive Screw, M3 x 0.5 mm Thread, 6mm Long	92095A179 MMC
0.246" Diameter Tight Tolerance Hardened 01 Tool Steel Rod	8893K202 MMC

*MMC = McMaster Carr

Appendix D - Wind Tunnel & Load Cell Calibration Test Procedure

The Static Module requires calibration of the load cells prior to wind tunnel test. All other parts have been made and have been tested to fit well together. The static module after assembly can be easily integrated into the rocket frame and is intended to fit as illustrated.

The wind tunnel we are planning to use is the Parkinson Wind Tunnel in UBC. The maximum safe operational wind speed is 30 m/s. The wind tunnel has an X-Y load balance and data is recorded off a dedicated computer.

The maximum recommended sample cross section area is 7% that of the wind tunnel. The cross section area of our prototype is only 3.06% that of the wind tunnel test section. The maximum side and drag force that can be experienced by the load cell is 250N in each X/Y direction and we are expected to be well below this upper bound.

At minimum the following data should be collected from the wind tunnel test:

Table 14: Minimum recommended windtunnel test conditions

Wind Speed (m/s)	AOA of Fin
30	0
30	10
20	10
10	10

Other data points that are valuable to have are different angles (0-15 degrees) at each wind speed increment. An interesting data point would also be to find the stall AOA at 30m/s of the canard and compare that to simulation results.

Calibration Test Procedure for Load Cell:

1. Assemble the aluminum block with load cells on each side and attach to the mounting plate.
2. Orient the mounting plate such that the normal axis is parallel with the horizontal and mimics the orientation in the wind tunnel as much as possible.
3. Run the test procedure with more weights to 500g.
4. Find the zero and plot a graph of Δ reading (comparing to initial value) against test weight.
5. The linear regression $y = mx + b$ will translate readings to weight. "b" will be the zero point and "m" is the scaling factor.
6. Immediately before each test, determine the current zero point "b".
7. Immediately after each test, record the current zero point "b" to find any hysteresis errors.

References

1. Wilson, A. (2019, October 24). Saab 37 Viggen. Retrieved Dec 31, 2019 from https://en.wikipedia.org/wiki/Saab_37_Viggen#/media/File:Saab_AJS-37_Viggen_37098_52 _(SE-DXN)_(9256079273).jpg.

2. Missile Control Systems. (n.d.). Retrieved Dec 31, 2019 from http://www.aerospaceweb.org/question/weapons/q0158.shtml.

3. Delft Aerospace Rocket Engineering. (n.d.). Advanced Control Team. Retrieved January 1, 2020 from https://dare.tudelft.nl/projects/advanced-control-team/.

4. Walker, D., & Walker, D. (2016, May 9). Canard Aerodynamics. Retrieved January 1, 2020 from http://www.cusf.co.uk/category/canards/.

5. Drag Force - Drag Equation. (n.d.). Retrieved January 3, 2020, from https://www.nuclear-power.net/nuclear-engineering/fluid-dynamics/what-is-drag-air-and-fluid -resistance/drag-force-drag-equation/.

6. Milligan, T. V. (2017, May 2). What is the best fin shape for a model rocket? *Peak of Flight*, (442). Retrieved January 2, 2020.

7. Strudwicke, C. (2009, May). Roll control of a Small Amateur Rocket. Retrieved January 3, 2020 from http://home.iprimus.com.au/sstrudwicke/Electronics/Roll_control_of_a_small_amateur_rocke t.pdf

8. Stall Angle. (n.d.). Retrieved January 3, 2020, from https://www.sciencedirect.com/topics/engineering/stall-angle.

9. Guerrero, Valeria Avila; Barranco, Angel; and Conde, Daniel, "Active Control Stabilization of High Power Rocket" (2018). Mechanical Engineering Senior Theses. 81. https://scholarcommons.scu.edu/mech_senior/81. Retrieved February 25, 2020.

10. Walker, D., & Hunt, H. (2016). *Model Rocket Guidance by Canards* (dissertation). Retrieved January 8, 2020.

11. Allen, Jerry M.: Parametric Fin-Body and Fin-Plate Database for a Series of 12 Missile Fins. NASA/TM-2001-210652, 2001. Retrieved January 3, 2020 https://ntrs.nasa.gov/archive/nasa/casi.ntrs.nasa.gov/20010020654.pdf

12. Kirsten Wind Tunnel (KWT). (2019, November 22). Retrieved January 3, 2020 from https://www.aa.washington.edu/AERL/KWT.

13. Guerrero, Valeria Avila; Barranco, Angel; and Conde, Daniel, "Active Control Stabilization of High Power Rocket" (2018). Mechanical Engineering Senior Theses. 81. https://scholarcommons.scu.edu/mech_senior/81. Retrieved March 9, 2020.

14. Blair, A. B. M., Allen, J. M., & Hernandez, G. M. (1983, June). Effect of Tail-Fin Span on Stability and Control Characteristics of a Canard-Controller Missile at Supersonic Mach Numbers. Retrieved March 9, 2020 from https://ntrs.nasa.gov/archive/nasa/casi.ntrs.nasa.gov/19830019688.pdf

15. Adriano Arcadipane: Roll gyro stabilised. (2013, July 3). Retrieved February 2020, from https://forum.ausrocketry.com/viewtopic.php?t=4131

16. Center of Pressure. (2015, May). Retrieved January 2020, from https://www.grc.nasa.gov/WWW/K-12/airplane/cp.html

17. Barrowman, J. (1988). Stability of a Model Rocket in Flight. Retrieved March 2020, from http://www.rockets4schools.org/images/Rocket.Stability.Flight.pdf

18. Longitudinal Vehicle (Pitch) Dynamics, Static and Dynamic Stability. (n.d.). Retrieved March 2020, from http://mae-nas.eng.usu.edu/MAE_5900_Web/5900/USLI_2010/Flight_Mechanics/Section5.2.pdf

19. Slosh dynamics. (2020, March 20). Retrieved April 3, 2020 from https://en.wikipedia.org/wiki/Slosh_dynamics

20. Launcher propellant slosh testing. (2013, July). Retrieved April 4, 2020 from https://www.esa.int/ESA_Multimedia/Videos/2013/ 07/Launcher_propellant_slosh_testing